https://doi.org/10.5194/tc-2023-156
Preprint. Discussion started: 9 October 2023

The Cryosphere Discussions
Open Access
EGU

The long–term sea–level commitment from Antarctica

Ann Kristin Klose[1,2], Violaine Coulon[3], Frank Pattyn[3], and Ricarda Winkelmann[1,2]

[1]FutureLab Earth Resilience in the Anthropocene, Earth System Analysis & Complexity Science, Potsdam Institute for Climate Impact Research (PIK), Member of the Leibniz Association, 14473 Potsdam, Germany
[2]Institute of Physics and Astronomy, University of Potsdam, 14476 Potsdam, Germany
[3]Laboratoire de Glaciologie, Université libre de Bruxelles (ULB), Brussels, Belgium

Correspondence: Ann Kristin Klose (annkristin.klose@pik-potsdam.de) and Ricarda Winkelmann (ricarda.winkelmann@pik-potsdam.de)

Abstract. The evolution of the Antarctic Ice Sheet is of vital importance given the coastal and societal implications of ice loss, with a potential to raise sea level by up to 58 m if melted entirely. However, future ice–sheet trajectories remain highly uncertain. One of the main sources of uncertainty is related to nonlinear processes and feedbacks of the ice sheet with the Earth System on different timescales. Due to these feedbacks and the ice–sheet inertia, ice loss may already be triggered in the next decades and then unfolds delayed on multi–centennial to millennial timescales. This committed Antarctic sea–level contribution is not reflected in typical sea–level projections based on mass balance changes of Antarctica, which often cover decadal–to–centennial timescales. Here, using two ice–sheet models, we systematically assess the multi–millennial sea–level commitment from Antarctica in response to warming projected over the next centuries under low– and high–emission pathways. This allows bringing together the time horizon of stakeholder planning with the much longer response times of the Antarctic Ice Sheet.

Our results show that warming levels representative of the lower–emission pathway SSP1-2.6 may already result in an Antarctic mass loss of up to 6 m sea–level equivalent on multi–millennial timescales. This committed mass loss is due to a strong grounding–line retreat in the Amundsen Sea Embayment as well as a potential drainage from the Ross Ice Shelf catchment and onset of ice loss in Wilkes subglacial basin. Beyond warming levels reached by the end of this century under the higher–emission trajectory SSP5-8.5, a collapse of the West Antarctic Ice Sheet is triggered in the entire ensemble of simulations from both ice–sheet models. Under enhanced warming, next to the marine parts, we also find a substantial decline in ice volume of regions grounded above sea level in East Antarctica. Over the next millennia, this gives rise to a sea–level increase of up to 40 m in our experiments, stressing the importance of including the committed Antarctic sea–level contribution in future projections.

1 Introduction

The future sea–level contribution from the Antarctic Ice Sheet, which stores enough ice to raise sea level by up to 58 m (Fretwell et al., 2013), is of vital importance for coastal communities ranging from small islands to the world's mega–cities, ecosystems and the global economy (Clark et al., 2016).

https://doi.org/10.5194/tc-2023-156
Preprint. Discussion started: 9 October 2023


The Cryosphere Discussions

The Antarctic Ice Sheet has experienced changing environmental conditions on various timescales from decadal to orbital–scale climate variability since its inception at the Eocene–Oligocene transition about 34 Mry ago (Zachos et al., 2001; DeConto and Pollard, 2003). This resulted in strong variations in its volume and extent linked to the slow multi–millennial changes in the Earth's astronomical configuration during the early to mid–Miocene (Naish et al., 2001; Levy et al., 2016) and the Pliocene (Naish et al., 2009; Pollard and DeConto, 2009). While large parts of the terrestrial East Antarctic Ice Sheet have persisted for millions of years (Sugden et al., 1995; Shakun et al., 2018), ice–sheet variability involved an occasional collapse of the West Antarctic Ice Sheet (Naish et al., 2009) and inward migration of ice–sheet margins in marine–based sectors of East Antarctica during Pliocene warm periods (Cook et al., 2013; Patterson et al., 2014; Aitken et al., 2016). During Pleistocene Interglacials, Antarctic ice loss contributed to sea–level high–stands (Wilson et al., 2018; Blackburn et al., 2020; Turney et al., 2020).

The future trajectory of the Antarctic Ice Sheet under progressing warming, however, is highly uncertain. This is due to uncertainties in the (representation of) ice–sheet processes and ice–climate interactions (Fox-Kemper et al., 2021) as well as the potentially high magnitudes and rates of recent and projected warming. The present rate of warming is unprecedented in at least 2000 years (Gulev et al., 2021). The amount of warming projected for the end of this century under the Shared Socioeconomic Pathways (e.g., for the higher–emission scenario SSP5-8.5 with an increase in global annual mean surface air temperature of 3.6 °C to 6.5 °C relative to 1850 – 1900; Lee et al., 2021) is comparable to the transition from the Last Glacial Maximum to the beginning of the Holocene, but is expected to develop on much shorter timescales.

At present, accelerated mass loss of the Antarctic Ice Sheet is concentrated in West Antarctica and the East Antarctic Wilkes land (Otosaka et al., 2023; Rignot et al., 2019; Li et al., 2016; Miles et al., 2021), likely driven by ocean–induced melting due to the intrusion of warm water into the ice–shelf cavities (Paolo et al., 2015). In future projections so far, for instance provided by the recent Ice Sheet Model Intercomparison Project ISMIP6 (Seroussi et al., 2020; Payne et al., 2021), the transient sea–level response to the projected warming ranges from a slight mass gain to a mass loss of Antarctica by the end of this century under multiple emission scenarios (with the largest spread in sea–level change given by higher–emission pathways RCP8.5 and SSP5-8.5). The bulk of sea–level rise, however, is expected to unfold beyond the end of this century (Clark et al., 2016; Fox-Kemper et al., 2021) due to (1) the inertia of the continental–scale ice sheet in combination with (2) the potential of crossing critical thresholds with ongoing global warming. This long–term sea–level response, that has already been triggered or may be triggered during the next decades (but unfolds over the following centuries and millennia), might be substantially higher than and is not represented in typical sea–level projections. Here, we assess this expected long–term committed sea–level change, by stabilizing the climatic boundary conditions at specific points in time and letting the ice sheet evolve over several millennia. We furthermore identify the gap between the transient *realized* sea–level contribution from Antarctica at a particular point in time and the respective long–term *committed* sea–level contribution (Winkelmann et al., in review).

The slow ice–sheet response to perturbations in its climatic boundary conditions owing to high inertia results in a time–lag between forcing and the resulting mass change. As the ice–sheet response unfolds on centennial to multi–millennial timescales, sea–level will keep rising for millennia to come even if warming is kept on a constant level (Golledge et al., 2015; Winkelmann et al., 2015). This is especially due to the softening–induced increase in the creep component of the ice flow and internal feedbacks (Golledge et al., 2015; Clarke et al., 1977).

https://doi.org/10.5194/tc-2023-156
Preprint. Discussion started: 9 October 2023

In addition, the Antarctic Ice Sheet is subject to several positive (and negative) feedback mechanisms determining its long–term stability (Fyke et al., 2018; Garbe et al., 2020). For example, accelerated ice loss may be triggered once the self–reinforcing surface melt–elevation feedback (Levermann and Winkelmann, 2016; Oerlemans, 1981) kicks in. With the lowering of the ice–sheet surface due to melting, it is exposed to higher air temperatures owing to the atmospheric lapse rate. Surface melting is, in turn, enhanced, promoting persistent ice loss upon crossing a critical threshold. Furthermore, the marine parts of the ice sheet, e.g., in West Antarctica or the Aurora and Wilkes subglacial basins in East Antarctica, are found to be susceptible to self–sustained, potentially irreversible grounding–line retreat (Garbe et al., 2020; Rosier et al., 2021; Mengel and Levermann, 2014; Feldmann et al., 2014). The rapid grounding–line retreat is often associated with a self–amplifying feedback in which the increased ice flow across the grounding line caused by an initial retreat fosters further retreat. In a theoretical flowline setup, it was shown that, due to the ice flux being a nonlinear function of the ice thickness, grounding lines of ice sheets grounded below sea level on a retrograde, inland sloping bed are unstable (Marine Ice Sheet Instability; Weertman, 1974; Schoof, 2007). More complex stability conditions arise in three dimensions when accounting for additional processes such as, e.g., buttressing (Gudmundsson et al., 2012; Haseloff and Sergienko, 2018; Pegler, 2018), calving and submarine melting (Haseloff and Sergienko, 2022) or the presence of feedbacks between the ice sheet and its environment (Sergienko, 2022). Ice loss may be dampened, on the other hand, by negative feedbacks such as introduced by e.g., the isostatic rebound of the solid Earth underlying the ice sheet to ice mass changes, which could potentially stabilize West Antarctic grounding lines (Coulon et al., 2021; Barletta et al., 2018).

Depending on the interplay of these feedbacks, persistent mass loss may be triggered once critical forcings or tipping points (Lenton et al., 2008; Armstrong McKay et al., 2022), for instance in temperature, are crossed. The Antarctic Ice Sheet was therefore classified as a tipping element of the climate system (Lenton et al., 2008; Armstrong McKay et al., 2022). Due to the inertia in the system and the related delay in the ice–sheet response under realistic forcing, the ice sheet's trajectory likely deviates from the ice–sheet equilibrium response to warming (Garbe et al., 2020; Rosier et al., 2021). While consequences of self–sustained ice loss potentially triggered in the next decades may play out and become visible over millennial timescales (Reese et al., 2023) (characterized as a slow onset of tipping; Ritchie et al., 2021), tipping may be sped up by forcing beyond the critical threshold. For the Greenland Ice Sheet, it was shown that the timescales of ice–sheet decline strongly depend on how far its critical temperature threshold is exceeded (Robinson et al., 2012).

Previous assessments of the long–term contribution to sea–level rise from the Antarctic Ice Sheet have been primarily restricted to a single ice–sheet model and have rarely explored intra– and inter–model uncertainties as well as uncertainties in climate forcing (Golledge et al., 2015; Clark et al., 2016): They suggest that the grounding lines in the Amundsen Sea Embayment may at present already be undergoing or may be committed to a self–amplified retreat under sustained present–day climate conditions until a new stable geometric configuration is reached (Reese et al., 2023; Joughin et al., 2014; Favier et al., 2014; Seroussi et al., 2017; Arthern and Williams, 2017; Golledge et al., 2019, 2021). The potential for pronounced grounding–line recession in marine–based portions of West Antarctica and the Wilkes subglacial basin in East Antarctica until the end of the millennium (Golledge et al., 2015; Clark et al., 2016; Winkelmann et al., 2015; Bulthuis et al., 2019; Chambers et al., 2022; Coulon et al., 2023) was illustrated for higher–emission scenarios, giving rise to an Antarctic mass loss of multiple

https://doi.org/10.5194/tc-2023-156
Preprint. Discussion started: 9 October 2023

meters of sea–level equivalent. On multi–millennial timescales, the loss of the portion of the ice sheet grounded above sea level in East Antarctica may be locked in for strong atmospheric warming, which would eventually commit the Antarctic Ice Sheet to contribute several tens of meter to global mean sea–level rise (Clark et al., 2016; Winkelmann et al., 2015).

Here we systematically study the long–term multi–millennial evolution of the Antarctic Ice Sheet in response to a wide range of possible future climate trajectories and thereby quantify its sea–level commitment for stabilized climate at different points in time over the course of the next centuries taking into account uncertainties in climatic boundary conditions and ice–sheet processes, by means of two different ice–sheet models: PISM (Bueler and Brown, 2009; Winkelmann et al., 2011) and Kori-ULB (previously called f.ETISh; Pattyn, 2017). The remainder of this paper is structured as follows: In the following Sect. 2 we describe the methods for performing sea–level projections on multi–millennial timescales. Results are presented in Sect. 3 and discussed in Sect. 4 with a focus on different sources of uncertainties, arising from the divergence of future climate trajectories as well as structural uncertainties, distinct initialisations and certain processes and their parameterisations in ice–sheet models.

2 Methods

2.1 Ice–sheet models

2.1.1 PISM

The Parallel Ice Sheet Model (PISM; Bueler and Brown, 2009; Winkelmann et al., 2011) is an open–source, thermo–mechanically–coupled ice sheet/stream/shelf model. In hybrid mode, the shallow–ice approximation (SIA) and shallow–shelf approximation (SSA) are solved and superimposed, giving rise to different dynamic regimes from the slow–flowing ice in the ice–sheet interior to the faster–flowing streams and ice shelves. We here use a modified version of PISM release v1.0 (Garbe et al., 2020). In particular, centered differences of the ice thickness across the grounding line are calculated to derive the surface gradient, which have been shown to improve the representation of the driving stress at the grounding line (Reese et al., 2023). We use a rectangular grid of 16 km horizontal resolution and a vertical grid structure with the highest resolution at the base of the ice sheet and shelves.

Basal shear stress τ_b and shallow–shelf approximation basal sliding velocities u_b are related in a general power law of the form

$$\tau_b = -\tau_c \frac{u_b}{u_{th}^q |u_b|^{1-q}} \tag{1}$$

with the threshold velocity $u_{th} = 100$ m yr^{-1} and the sliding exponent q. The yield stress τ_c is determined by the Mohr–Coulomb failure criterion (Cuffey and Paterson, 2010) as

$$\tau_c = \tan(\phi N_{\text{till}}) \tag{2}$$

including the till friction angle ϕ and the effective pressure N_{till}. The till friction angle is parameterized as piecewise linear with bed elevation (Martin et al., 2011) in our simulations with a lower value of 24° for topography below -700 m and an upper

https://doi.org/10.5194/tc-2023-156
Preprint. Discussion started: 9 October 2023


The Cryosphere Discussions

value of 30° for topography above 500 m (following Reese et al., 2023). The effective pressure $N_{\rm till}$ in PISM is a function of the overburden pressure P_0 and the fraction of the effective water thickness in the till layer $s = W_{\rm till}/W_{\rm max}$:

$$N_{\rm till} = \min\{P_0, N_0\Big(\frac{\delta P_0}{N_0}\Big)^s 10^{(e_0/C_c)(1-s)}\} \tag{3}$$

where the values for the constants N_0, e_0 and C_c are chosen following Bueler and van Pelt (2015). The amount of water from basal melt in the till layer $W_{\rm till}$ with a maximum of $W_{\rm max} = 2$ m evolves according to the non–conserving 'null' hydrology model (as described in Bueler and van Pelt, 2015) with a decay rate C of water in the till. The grounding–line position is simulated at a subgrid scale evolving freely without imposing additional flux conditions. Basal resistance is linearly interpolated on a sub–grid scale around the grounding line (Feldmann et al., 2014), while sub–shelf melt in partially floating cells is not applied in the experiments presented here. We apply eigencalving, which linearly relates the calving rate to the spreading rate tensor with a proportionality factor of $K = 1\text{x}10^{17}$ m s (Levermann et al., 2012). Additionally, thin ice below 50 m is removed at the calving front (thickness calving) and a maximum extent for ice shelves is defined (Garbe et al., 2020; Albrecht et al., 2020). Our simulations include the effect of the viscous and elastic response of the bedrock to changes in ice load, following Lingle and Clark (1985) and Bueler et al. (2007), with an upper mantle viscosity $\eta = 1\text{x}10^{21}$ Pa s and density $\rho = 3300$ kg m^{-3} as well as a flexural rigidity of the lithosphere of $5\text{x}10^{24}$ N m.

2.1.2 Kori-ULB

The Kori-ULB ice flow model, which is the follow–up of the f.ETISh model (Pattyn, 2017), is a vertically–integrated, thermo–mechanically–coupled hybrid ice–sheet/ice–shelf model, and incorporates relevant features for studying the evolution of the Antarctic Ice Sheet such as the mass balance–elevation feedback, basal sliding, sub–shelf melting, calving, and bedrock deformation. The ice flow is governed by a combination of the shallow–ice (SIA) and shallow–shelf (SSA) approximations for grounded ice and by the shallow–shelf approximation for floating ice shelves (Bueler and Brown, 2009; Winkelmann et al., 2011). Simulations of the multi–millennial Antarctic sea–level contribution presented here were performed with Kori-ULB version 0.91 at a horizontal resolution of 16 km.

Basal sliding is parameterized using a Weertman sliding law, i.e.,

$$\tau_b = A_b^{-1/m} |\mathbf{v}_b|^{1/m-1} \mathbf{v}_b \tag{4}$$

where τ_b and $\mathbf{v}_b$ are the basal shear stress and the basal velocity, respectively, and with a basal sliding exponent $m = 3$. The values of the basal sliding coefficient A_b are inferred following the nudging method of Pollard and DeConto (2012b) and Bernales et al. (2017).

At the grounding line, a flux condition (related to the ice thickness at the grounding line; Schoof, 2007) is imposed as in Pollard and DeConto (2012a) and Pollard and DeConto (2020) to account for grounding–line migration. This implementation can reproduce the steady–state behavior of the grounding line and its migration (Schoof, 2007) also at coarse resolution (Pattyn et al., 2013). Using this flux condition, the marine ice–sheet behavior in Antarctica was simulated by large–scale ice–sheet models (Pollard and DeConto, 2012a; DeConto and Pollard, 2016; Pattyn, 2017; Sun et al., 2020), with similar results under

https://doi.org/10.5194/tc-2023-156
Preprint. Discussion started: 9 October 2023

buttressed conditions as in high–resolution models (Pollard and DeConto, 2020). Calving at the ice front depends on the parameterized combined penetration depths of surface and basal crevasses relative to the total ice thickness. Similar to Pollard et al. (2015) and DeConto and Pollard (2016), the parameterisation of the crevasse penetration depths involves the divergence of the ice velocity, the accumulated strain, and the ice thickness. Bedrock adjustment in response to changes in ice and ocean load is taken into account by means of the commonly used Elastic Lithosphere–Relaxed Asthenosphere (ELRA) model, where the solid–Earth system is represented by a relaxing viscous asthenosphere below a thin elastic lithosphere plate (Le Meur and Huybrechts, 1996; Coulon et al., 2021). A spatially uniform relaxation time of 3000 years and a flexural rigidity of the lithosphere of 10^{25} N m is chosen in the simulations presented here.

2.2 Experimental design

2.2.1 Assessing Antarctic sea–level commitment

We aim to determine the long–term multi–millennial sea–level contribution from the Antarctic Ice Sheet and thereby its sea-level commitment using the ice–sheet models PISM and Kori-ULB (compare Sect. 2.1). After initializing the models to obtain initial Antarctic Ice Sheet configurations and running historical simulations (described in more detail in the following Sect. 2.2.2 and 2.2.3, and illustrated in Figure 1), we assess the response of the Antarctic Ice Sheet to changes in the oceanic and atmospheric boundary conditions derived from state–of–the–art climate model projections available from the sixth phase of the Coupled Model Intercomparison Project (CMIP6) under the Shared Socioeconomic Pathways SSP1-2.6 and SSP5-8.5 (thereby covering a wide range from lower– to higher–emission scenarios). As we are interested in the long–term response, we focus on a set of CMIP6 General Circulation Models (GCMs) that provide forcing until the year 2300. Thereby, we obtain the transient *realized* sea–level contribution of the Antarctic Ice Sheet at given points in time (for instance, in the year 2100, filled dots in Figure 1). We then quantify the long–term *committed* sea–level contribution by stabilizing forcing conditions of the climate trajectories at regular intervals in time ('branching off' in the years 2050, 2100, 2150, 2200, 2250 and 2300) and letting the ice sheet evolve over several millennia (until year 7000) under fixed climatic boundary conditions characteristic for the respective branchoff year (Fig. 1, open dots). Climate conditions of the distinct branchoff years are determined as the mean over the previous ten years before the branchoff.

2.2.2 initialisation

Both ice sheet models are initialized using constant climatic boundary conditions representing the year 1950 (Fig. 1). More specifically, 'historic' climatic boundary conditions for the year 1950 are constructed using the historic changes in ocean and atmosphere with respect to the reference period from 1995 to 2014 from the Norwegian Earth System Model (NorESM1-M; Bentsen et al., 2013). The oceanic and atmospheric anomalies are averaged over the period 1945–1955 and subsequently added to present–day atmospheric temperatures and precipitation as well as observed present–day ocean temperatures and salinities. Two distinct present–day atmospheric climatologies are derived from the Regional Climate Models (RCMs) Modèle Atmosphérique Régional (MARv3.11; Kittel et al., 2021) and Regional Atmospheric Climate MOdel (RACMO2.3p2; Van Wessem

https://doi.org/10.5194/tc-2023-156
Preprint. Discussion started: 9 October 2023

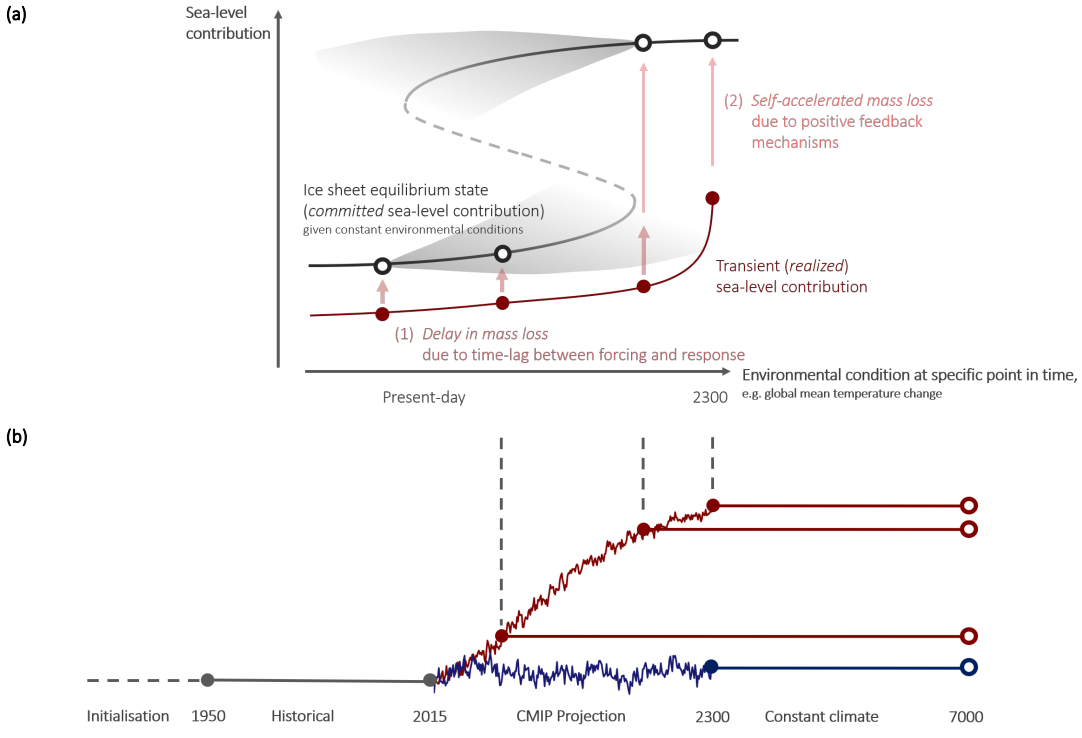

Figure 1. Schematic of the experimental design (a): Idealized and simplified stability diagram of the Antarctic Ice Sheet as possible tipping element, which illustrates some underlying factors potentially contributing to a gap between the transient realized and long–term committed ice–sheet response (in terms of sea–level contribution). (b): Schematic summary of the experimental design used for assessing the long–term committed contribution from the Antarctic Ice Sheet to sea–level rise with the ice–sheet models PISM and Kori-ULB. Starting with the initialisation of the ice–sheet models to build ice–sheet representations in 1950, historical simulations are run until 2015 (present–day). Using potential future climate trajectories based on CMIP6, the transient realized Antarctic sea–level change is projected until the year 2300. Additional simulations branching off at regular intervals in time determine the sea–level commitment under stabilized climatic boundary conditions sustained over several millennia.

https://doi.org/10.5194/tc-2023-156
Preprint. Discussion started: 9 October 2023

et al., 2018) to take into account uncertainties in the representation of present–day Antarctic surface climate (compare Mottram et al., 2021). Both present–day atmospheric climatologies are involved in the initialisation of each ice–sheet model, resulting in four (initial) ice–sheet model configurations. For ocean temperatures and salinities, present–day observations based on Schmidtko et al. (2014) are used.

To build initial ice–sheet representations with PISM, a spin–up approach is applied for each of the atmospheric climatologies individually. Uncertainties in ice–sheet model parameters are taken into account by running an ensemble of spin–up simulations and choosing the initial state which fits well to observations of present–day ice thickness, ice velocities and grounding–line position. More specifically, starting from Bedmap2 ice thickness and topography (Fretwell et al., 2013), PISM is run for 600 000 years with constant geometry to obtain a thermodynamic equilibrium. Applying the constant historic boundary conditions associated with the year 1950, an ensemble of simulations with varying model parameters (guided by recent PISM ensembles; Reese et al., 2023; Albrecht et al., 2020) is run for several thousand years. Here, we include the SIA enhancement factor ($E_{SIA} \in 1.5, 2$; varied around the reference value of Albrecht et al., 2020) and parameters related to basal sliding, namely the pseudo–plastic sliding exponent ($q \in 0.25, 0.5, 0.75$, within the range investigated by Albrecht et al., 2020; Lowry et al., 2021), the till effective overburden fraction ($\delta \in 1.5, 2.0, 2.5$; Bueler and van Pelt, 2015) and the decay rate of till water content ($C \in 7, 10$ mm yr^{-1}, equivalent to the range explored by Albrecht et al., 2020). After 5000 years of simulation, the ensemble members are assessed with a scoring method following Albrecht et al. (2020) and Reese et al. (2020). The scoring method is based on the mean–square–error mismatch of grounded and floating ice area, ice thickness, grounding–line location and surface velocity compared to present–day observations (Fretwell et al., 2013; Rignot et al., 2011). Each indicator is evaluated for the entire Antarctic domain as well as for the Amundsen, Filchner–Ronne and Ross regions individually. The five best–scoring ensemble members in terms of the continental as well as the basin–scale indicators are continued until reaching 50 000 years of simulation, and experiments are performed with the ice–sheet configuration performing well in the scoring after 50 000 years.

For Kori-ULB, ice–sheet initial conditions and basal sliding coefficients are obtained in an inverse simulation following Pollard and DeConto (2012b) for each of the 'historic' atmospheric climatologies associated with the year 1950 (as described above). In this inverse procedure, the difference to the observed ice thickness (Bedmachine; Morlighem et al., 2020) is minimized by iteratively adjusting the basal sliding coefficients under grounded ice and sub–shelf melt rates under floating ice (Bernales et al., 2017). The resulting sub–shelf melt rates may therefore be interpreted as balance sub–shelf melt rates and are independent of the oceanic boundary conditions (forcing), while the ice–sheet states are in steady–state with the initial atmospheric climatologies. Applying constant historic ocean and atmospheric boundary conditions associated with the year 1950, a short relaxation is run for 10 years after the model initialisation and before the historical simulation. This limits an initial shock that may results from the transition from the balance sub–shelf melt rates derived during the transient spin–up to the imposed sub–shelf melt parameterisation scheme. The two initial ice–sheet states resulting from the nudging spin–ups are therefore in quasi–equilibrium. They compare well to the observed ice dynamics, ice geometry, and grounding–line position (compare Fig. S1), and are within the range of the ISMIP6 models (Seroussi et al., 2019).

https://doi.org/10.5194/tc-2023-156
Preprint. Discussion started: 9 October 2023

2.2.3 Forcing and boundary conditions over the historical period and until 2300

Starting from the initial ice–sheet configurations and climate conditions of the year 1950 described above, we run historical simulations for the time period from 1950 to 2015 (Fig. 1). Changes in oceanic and atmospheric conditions are derived from NorESM1-M, as recommended within ISMIP6 (Barthel et al., 2020; Nowicki et al., 2020). The corresponding ice–sheet response (as determined by PISM and Kori-ULB) over the historical period is shown in Figure S2. The atmospheric and oceanic forcing conditions until the year 2300, which are applied to the ice–sheet models for studying the future evolution of the Antarctic Ice Sheet, rely on a subset of state–of–the–art GCM projections available within CMIP6 (MRI-ESM2-0, UKESM1-0-LL, CESM2-WACCM, and IPSL-CM6A-LR). We apply climate forcing under both the Shared Socioeconomic Pathways SSP5-8.5 and SSP1-2.6. The selection of CMIP6 GCMs was guided by the limited availability of extended climate projections until 2300 within ScenarioMIP (O'Neill et al., 2016), while the climate sensitivity of the available GMCs (Meehl et al., 2020) and their performance in comparison with observations (e.g., Beadling et al., 2020; Purich and England, 2021; Bracegirdle et al., 2020) were considered as secondary criteria.

Following Nowicki et al. (2020), spatially–varying atmospheric (*near–surface air temperature*) as well as oceanic (*salinity* and *temperature*) anomalies with respect to the 1995–2014 mean climatology are directly derived from NorESM1-M over the historical period as well as from projections of the selected CMIP6 GCMs until the year 2300. Note that, for *precipitation*, ratios (instead of anomalies) with respect to the 1995–2014 mean precipitation are determined to avoid 'negative' absolute precipitation (e.g., Goosse et al., 2010, Equation 30). The respective anomalies are added to the present–day climatologies for the atmosphere (MAR, RACMO) and the ocean (Schmidtko et al., 2014). Thus, the resulting forcing matches present–day conditions in the 1995–2014 reference period (as in Reese et al., 2023). For the oceanic properties, yearly averaged forcing is applied to the ice–sheet models. Missing values for the oceanic forcing on the continental shelf (arising due to the coarse resolution of CMIP6 GCMs) and in currently ice–covered regions are filled following Kreuzer et al. (2021), i.e., by averaging over all existing values in neighbouring cells. In contrast, monthly forcing is used at the interface of the ice sheet to the atmosphere (as in Golledge et al., 2019).

Surface melt and runoff are determined from monthly atmospheric temperature and precipitation (i.e., accounting for the seasonal cycle) using a positive–degree–day (PDD) scheme (Reeh, 1991). The amount of PDD follows the approach presented in Calov and Greve (2005), with a default value for the standard deviation of $\sigma = 5$ °C and $\sigma = 4$ °C for PISM and Kori-ULB, respectively. Snow accumulation rates are derived from precipitation via an atmospheric temperature threshold with a linear transition between snow and rain. In Kori-ULB, natural variability is considered when determining snow accumulation rates (similar to the calculation of the amount of positive–degree–days) using a standard deviation of $\sigma = 3.5$ °C. Melt coefficients of 3 mm w.e. per PDD for snow and 8 mm w.e. per PDD for ice are used in both ice–sheet models after a comparison to MAR estimates until the year 2100 (Kittel et al., 2021; Coulon et al., 2023). A constant fraction of surface melt refreezes in PISM (Reeh, 1991), while Kori-ULB applies a simple thermodynamic parameterisation of the refreezing process (Huybrechts and De Wolde, 1999; Coulon et al., 2023). Computing surface melt and runoff in a PDD approach follows Garbe et al. (2020) and DeConto et al. (2021), likewise studying the future Antarctic response to changing environmental conditions and the ice–sheet

https://doi.org/10.5194/tc-2023-156
Preprint. Discussion started: 9 October 2023

stability on multi–millennial timescales. Applying the surface mass balance determined by RCMs, which are in turn forced by climate projections of GCMs, would be an alternative approach for projecting Antarctic sea–level change. However, surface mass balance estimates from RCMs are not yet available beyond the end of this century and may be biased by the use of a static ice–sheet geometry neglecting, for example, the surface melt–elevation feedback (Kittel et al., 2021).

To account for the **surface melt–elevation feedback**, the near–surface air temperature is corrected for changes in ice–sheet surface elevation. More specifically, air temperatures T_{forcing} provided to the ice–sheet models are shifted linearly with a change in surface elevation Δh as

$$T = T_{\text{forcing}} + \Gamma \Delta h \tag{5}$$

following the atmospheric lapse rate Γ of 8°C / km.

Sub–shelf melt rates are computed by using the Potsdam Ice–shelf Cavity mOdel (PICO; Reese et al., 2018). PICO calculates sub–shelf melt rates from far–field salinities and temperatures and parameterizes the overturning circulation in ice–shelf cavities. Ocean properties derived from CMIP6 GCMs are linearly interpolated to the continental shelf depth (Kreuzer et al., 2021) to be applicable to PICO. The overturning strength parameter $C = 3\text{x}10^{6}$ m^{6} s^{-1} kg^{-1} and the turbulent heat exchange coefficient $\gamma_T^* = 7\text{x}10^{-5}$ m s^{-1} (with correction of ocean properties of Schmidtko et al. (2014) to match observed present–day melt rates from Adusumilli et al. (2020)) are used for PISM experiments, as they have been found to fit melt sensitivities well (Reese et al., 2023). For Kori-ULB experiments, the overturning strength and the turbulent heat exchange coefficient are chosen as $C = 1\text{x}10^{6}$ m^{6} s^{-1} kg^{-1} and $\gamma_T = 4\text{x}10^{-5}$ m s^{-1}, respectively.

3 Results

We here present the transient response of the Antarctic Ice Sheet to a range of possible future climate trajectories until the year 2300 (Sect. 3.1) along with the associated committed ice–sheet evolution on multi–millennial timescales (Sect. 3.2). The dependency of the committed sea–level contribution on the environmental conditions in Antarctica sustained over several thousands of years after their stabilization at different points in time during the next centuries is assessed in Sect. 3.3.

3.1 Transient ice–sheet response until 2300

Following the **lower–emission pathway SSP1-2.6** results in a sea–level change ranging from -5.0 cm to +8.0 cm by the end of this century and from -0.2 m to +0.5 m in 2300 (Fig. 2a; Tab. 1). Therein, Kori-ULB projects a positive sea–level contribution for this lower–emission scenario (dashed lines), while PISM projects a sea–level drop (solid lines). The overall sign of ice–sheet mass changes contributing to a change in sea–level depends on the balance between the dynamic response to sub–shelf melting and ice–shelf thinning and the surface mass balance. We find that the integrated surface mass balance remains positive for both ice–sheet models until 2300 under SSP1-2.6 (Fig. S3a). However, the response in dynamic discharge contributing to a sea–level increase on centennial timescales is higher in Kori-ULB (with ice–sheet thinning in the Amundsen Sea Embayment

https://doi.org/10.5194/tc-2023-156
Preprint. Discussion started: 9 October 2023

285 extending inland, Fig. S4–S5) than in PISM (see Fig. S6–S7 for comparison), explaining the diverging sea–level contribution under SSP1-2.6 until 2300.

Under climate trajectories following the **SSP5-8.5 emission pathway**, the Antarctic ice loss varies between -6.0 cm and +6.0 cm sea–level equivalent by the end of this century, increasing to +0.7 – +3.1 m by 2300 (Fig. 2b; Tab. 1). The initial sea–level drop by 2100 is again found in simulations from PISM and can be attributed to increasing snowfall with warming, which 290 dominates the ice–sheet mass balance until the end of this century. Simulations by Kori-ULB show an earlier grounding–line retreat in the Amundsen Sea Embayment, outweighing the initial increase in the integrated surface mass balance and resulting in a positive sea–level contribution already during the 21st century. Beyond 2100 and over the course of the following two centuries, the grounding line in the Amundsen Sea Embayment may retreat substantially (Fig. 3b, realized) depending on the sensitivity of the initial state to the imposed ocean warming (being strongest under IPSL-CM6A-LR and UKESM1-0-LL; 295 Fig. S8–S11 show the individual ice–sheet response determined by both ice–sheet models to the different centennial climate trajectories). At the same time, the integrated surface mass balance starts to decrease and may even turn negative for strong atmospheric warming (Fig. S3b). The major ice shelves including the Ross Ice Shelf as well as the Filchner–Ronne Ice Shelf thin, in particular near the grounding line, and are (in PISM only) even lost sequentially by 2150 and 2300, respectively (Fig. 3b, realized; Fig. S10–S11). As a consequence of reduced buttressing, the grounding line in the Siple Coast region starts to show 300 retreat.

Overall, the global mean sea–level contribution due to mass balance changes of the Antarctic Ice Sheet projected by PISM and Kori-ULB on centennial timescales (Fig. 2a and b; Tab. 1) is within the range of recent estimates: by the end of this century, estimates by the Ice Sheet Model Intercomparison Project ISMIP6 range from -9 cm to +30 cm under higher–emission pathways and from -1.4 cm to +15.5 cm under lower–emission pathways (Seroussi et al., 2020; Payne et al., 2021). The forced 305 response of the Antarctic Ice Sheet until 2300 is in line with the results of both Golledge et al. (2015) and Chambers et al. (2022) and is consistent with the range of -0.3 m – +3.2 m sea–level equivalent given as estimate for the Antarctic sea–level contribution in the latest IPCC assessment (Fox-Kemper et al., 2021).

3.2 Long–term committed ice–sheet evolution over the next millennia

Oceanic and atmospheric warming projected for the upcoming centuries may trigger changes in the dynamics and geometry 310 of the Antarctic Ice Sheet that are not realized on the same timescales (as the forcing), but unfold thereafter over the course of the following millennia, due to ice–sheet inertia and nonlinear feedbacks. After determining the transient realized sea–level response over the next centuries (Sect. 3.1), we investigate this long–term committed evolution of the Antarctic Ice Sheet by keeping environmental conditions constant at different points in time and letting the ice sheet evolve over several millennia (see Sect. 2.2.1).

315 Our simulations confirm that sea level may keep rising for centuries to millennia to come even if warming is kept at a constant level (Fig. 2c and d, consistent with, e.g., Winkelmann et al., 2015; Van Breedam et al., 2020). The delayed response of the Antarctic Ice Sheet on millennial timescales gives rise to a substantial gap between the transient *realized* (described in the previous Sect. 3.1) and the long–term *committed* Antarctic sea–level contribution, being more than the 100 (10)–fold of the

https://doi.org/10.5194/tc-2023-156
Preprint. Discussion started: 9 October 2023

sea–level change projected by the year 2100 (2300) (compare Figure 2a – d; Tab. 1). This commitment gap (Winkelmann et al., in review) depends on the specific climate trajectory and the warming levels that are reached at the respective (branchoff) point in time.

We find a sharp increase in the Antarctic sea–level contribution over the next millennium, irrespective of the emission scenario. When following the **lower–emission pathway SSP1-2.6**, the ice–sheet response levels off after a peak in the rate of Antarctic ice loss within this millennium or at latest by the beginning of the following millennium. It then stabilizes at qualitatively different stages of ice–sheet decline (Fig. 2c and e). In some cases, abrupt changes in the Antarctic sea–level contribution occur delayed (compared to other trajectories under the lower–emission pathway) in PISM, with a lag of multiple millennia to the onset of the perturbation in ice–sheet boundary conditions. These ice–sheet trajectories, however, eventually converge to the same magnitude of sea–level contribution on multi–millennial timescales. In our simulations under SSP1-2.6, we do not find a strong dependency of the long–term ice–sheet configuration reached in year 7000 on the point in time after which climatic boundary conditions are kept constant (Fig. 2e; Fig. 3a, committed). When sustaining the warming level potentially reached until year 2050, global mean sea–level may increase by +0.4 m to +3.8 m on the long–term (Fig. 2e; Tab. 1). For climatic boundary conditions representative of the end of this century and thereafter, Antarctic mass changes range between -0.2 m and +6.3 m of sea–level equivalent, which unfolds over the next millennia (Fig. 2e; Tab. 1). The applied GCM forcing determines the magnitude of the committed Antarctic sea–level contribution under SSP1-2.6 at a given (branchoff) point in time (Fig. 2e). For both ice–sheet models, stronger ocean warming in the Wilkes basin projected by UKESM1-0-LL and IPSL-CM6A-LR compared to the other GCMs may promote grounding–line retreat in this region (compare Fig. S12–S15), giving rise to the upper limit of long–term ice loss found under the lower–emission pathway (Fig. 2e). The magnitude of mass loss is further modulated by the consequences of a potential collapse of the Ross Ice Shelf as well as the extent of grounding–line recession in the Amundsen Sea Embayment. In PISM, a substantial portion of the marine ice–sheet in West Antarctica is lost by year 7000 under most considered climate trajectories (compare Fig. S14–S15), determining (in combination with a potential grounding–line retreat in the Wilkes basin) the upper range of Antarctic sea–level commitment under SSP1-2.6 in our ensemble of simulations (Fig. 2e). While the Ross Ice Shelf collapses under SSP1-2.6 in PISM, Filchner–Ronne Ice Shelf remains intact in most of these simulations (except for CESM2-WACCM). In Kori-ULB, grounding–line retreat is limited to Pine Island and Thwaites Glacier while both large ice shelves are preserved (with a slight grounding–line advance for Ross Ice Shelf, compare Fig. S12–S13). This limits the long–term sea–level change from Antarctica to approximately +3.0 m in Kori-ULB (in combination with a retreating grounding line in Wilkes basin under UKESM1-0-LL and IPSL-CM6A-LR; Fig. 2e).

Under the **SSP5-8.5 emission scenario**, the potential magnitude as well as the range of the long–term Antarctic sea–level response substantially increase with the point in time at which ocean and atmospheric warming is stabilized (Fig. 2f). Under the sustained warming levels potentially reached during the next decades (that is, by 2050) under this high–warming climate trajectory, long–term mass losses are projected to arise from marine regions in West Antarctica (Fig. 3b, committed), leading to +0.5 m – +3.7 m of global mean sea–level rise (comparable to changes under SSP1-2.6; Tab. 1). Fig. S16–S19 show the individual long–term ice–sheet response determined by both ice–sheet models to sustained warming levels reached by 2050 in the GCMs. Major portions of the catchment region of Thwaites and Pine Island Glaciers are drained in both ice–sheet models.

https://doi.org/10.5194/tc-2023-156
Preprint. Discussion started: 9 October 2023

In addition, the grounding line at the Siple Coast may retreat inland with a thinning of Ross Ice Shelf (or even a collapse, Fig. 3b, committed), as suggested in simulations by PISM. In response to changes in climatic boundary conditions projected for the end of this century, we find the committed sea–level contribution to be substantially larger (Fig. 2f): Marine parts of the West Antarctic Ice Sheet show a significant retreat (in some cases the West Antarctic Ice Sheet even collapses entirely), accompanied by a strong inland retreat of the grounding line in the East Antarctic Wilkes basin on the long term (depending on the climate forcing, Fig. 3b, committed; Fig. S16–S19). Compared to ice–sheet changes triggered within the next decades, this can lead to more than a doubling of the long–term mass loss ranging between +1.2 m and +8.5 m sea–level equivalent (by year 7000, Fig. 2f; Tab. 1). The mass loss until year 3000 amounts to +1.0 m – +4.9 m sea–level equivalent (compare Tab. 1), consistent with Chambers et al. (2022). For warming levels that are reached under SSP5-8.5 for any of the branchoff points after 2100, mass loss from Antarctica may continue well beyond the end of this millennium, with high rates of the Antarctic contribution to sea–level rise until the end of our simulations in year 7000 (Fig. 2d). This is due to additional and persistent ice loss in the Aurora, Wilkes and Recovery subglacial basins (Fig. 3b, committed). We also find a substantial ice thickness decrease in inner parts of East Antarctica grounded above sea level that is triggered under sustained high levels of warming and possibly exacerbated by the melt–elevation feedback (Fig. 3b, committed). In such cases, the long–term contribution of the Antarctic Ice Sheet to global mean sea–level rise may be as high as +40.8 m for sustained warming levels representative for the year 2300 (in the year 7000; with ice loss of +5.9 m – +31.7 m and +3.3 m – +13.8 m sea–level equivalent by the year 5000 and 3000, respectively, compare Tab. 1). Our upper range of long–term mass loss committed under constant climatic boundary conditions reached by the year 2300 is thus higher than previous estimates (under Representative Concentration Pathway RCP8.5, Golledge et al., 2015; Bulthuis et al., 2019), likely caused by higher magnitudes of imposed warming in the selected GCMs employed here.

In summary, comparing the long–term ice loss under both emission pathways, we find that the committed Antarctic sea–level contribution at a given point in time diverges beyond the end of this century (Fig. 2f, comparing projected multi–millennial ice loss under SSP5-8.5 to SSP1-2.6 indicated by light grey box). That is, the emission pathways become increasingly relevant for the long–term mass loss from Antarctica after 2100. At the same time, even the lower–emission scenario poses a considerable risk of Antarctic ice loss raising global mean sea–level by multiple meters over the next millennia. It should be noted that our simulations end in the year 7000. As a consequence, in some cases the ice sheet has not yet reached a new equilibrium with the sustained climatic boundary conditions yet. The complete loss of the East Antarctic Ice Sheet can thus not be ruled out on even longer timescales.

The growing spread of the Antarctic sea–level commitment for a given (branchoff) point in time is mainly caused by the divergence of the climate trajectories projected by the four GCMs (see discussion in Sect. 4.1). Under equivalent warming, the long–term dynamical and topographical changes of the Antarctic Ice Sheet are largely consistent (for each ice–sheet model configuration) and uncertainty in Antarctic ice loss for a given warming level is due to inter– and intra–model uncertainty (e.g., arising in the ice–sheet model initialisation, compare Sect. 2.2.2, and by differences between applied atmospheric climatologies). The relationship between the committed Antarctic mass changes and sustained warming as well as potential thresholds in the long–term ice–sheet response are further studied in the following Sect. 3.3.

https://doi.org/10.5194/tc-2023-156
Preprint. Discussion started: 9 October 2023

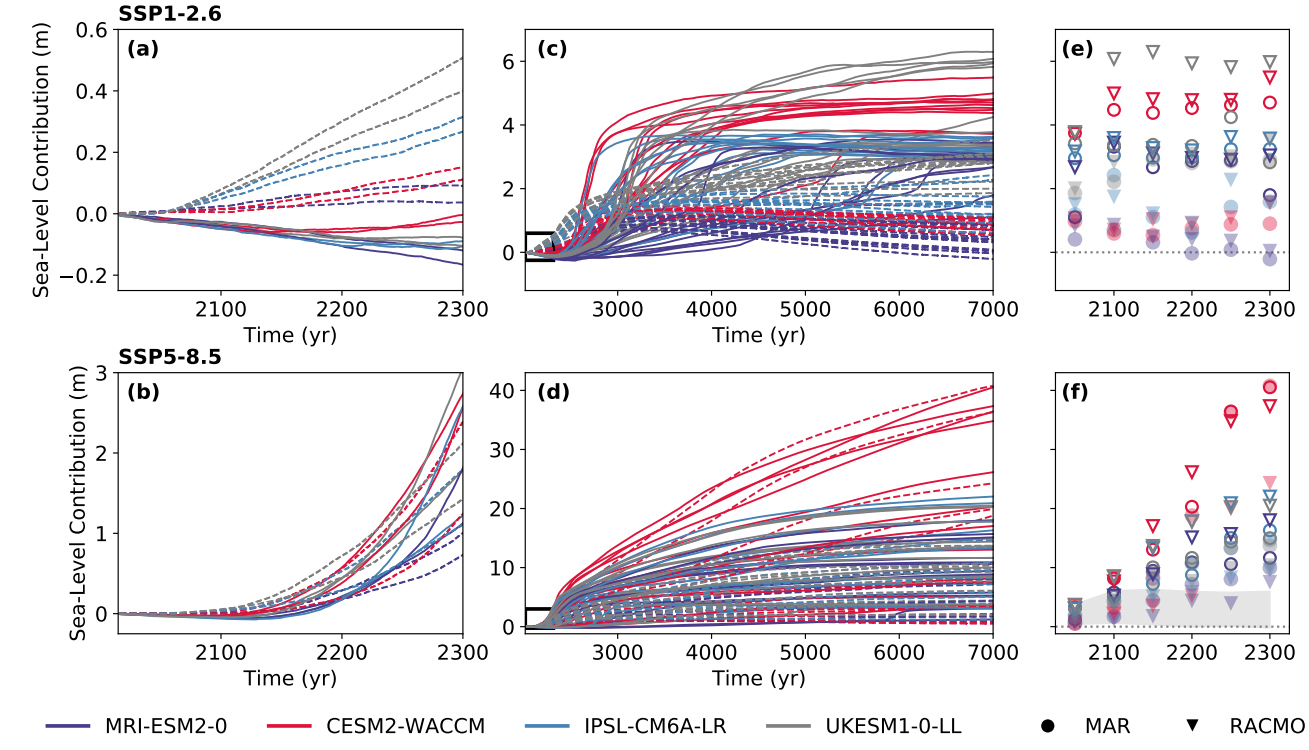

Figure 2. Projected ice loss from Antarctica on centennial to multi–millennial timescales (in meters sea–level equivalent) in response to changing climate conditions as projected by four different GCMs (given by the colour) under emission pathways SSP1-2.6 (upper row) and SSP5-8.5 (lower row), simulated by the ice–sheet models PISM (solid) and Kori-ULB (dashed). (a) and (b): Transient sea–level response from Antarctica until year 2300. (c) and (d): Multi–millennial Antarctic sea–level response until year 7000 to warming reached at different points in time throughout the next centuries. (e) and (f): Committed Antarctic sea–level contribution in the year 7000. Different atmospheric climatologies involved in the ice–sheet initialisation are indicated by the shape of the marker. Open and filled markers correspond to the long–term sea–level change determined by PISM and Kori-ULB, respectively. For comparison of the committed sea–level rise under both emission pathways, the range of long–term Antarctic ice loss by 7000 under SSP1-2.6 is indicated by the light grey box in (f).

https://doi.org/10.5194/tc-2023-156
Preprint. Discussion started: 9 October 2023

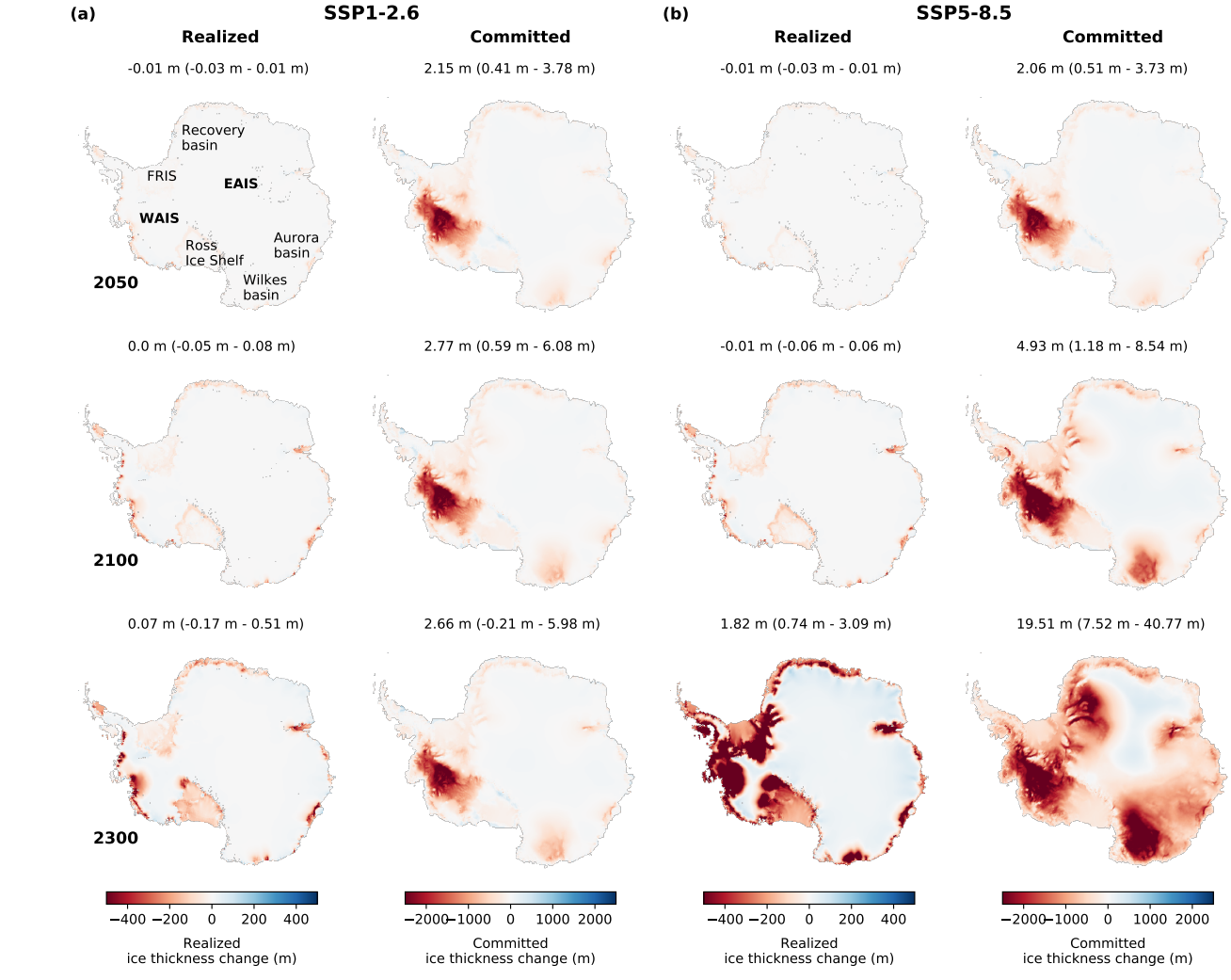

Figure 3. Realized and committed ice–sheet evolution following emission pathways SSP1-2.6 (a) and SSP5-8.5 (b). Shown is the mean thickness change for the realized and committed ice–sheet response (from left to right) when stabilizing climatic boundary conditions at different points in time (from top to bottom). EAIS, East Antarctic Ice Sheet; WAIS, West Antarctic Ice Sheet; FRIS, Filchner–Ronne Ice Shelf.

https://doi.org/10.5194/tc-2023-156
Preprint. Discussion started: 9 October 2023

Table 1. Mean, minimum and maximum value of the combined realized and committed ice loss (in meters sea–level equivalent) as determined by the ice–sheet models PISM and Kori-ULB under emission pathways SSP1-2.6 and SSP5-8.5. Ice loss is given for different points in time where climatic boundary conditions are stabilized. For a given point in time, upper rows represent SSP1-2.6 and lower rows correspond to SSP5-8.5.

		Realized	Committed in year 3000	Committed in year 5000	Committed in year 7000
2050	SSP1-2.6	-0.01	0.99	1.97	2.15
		(-0.03,0.01)	(-0.14,2.27)	(0.65,3.82)	(0.41,3.78)
	SSP5-8.5	-0.01	0.93	1.89	2.06
		(-0.03,0.01)	(-0.17,3.32)	(0.73,3.87)	(0.51,3.73)
2100	SSP1-2.6	0.00	1.32	2.57	2.77
		(-0.05,0.08)	(0.18,3.76)	(0.88,5.11)	(0.59,6.08)
	SSP5-8.5	-0.01	2.50	4.31	4.93
		(-0.06,0.06)	(0.98,4.87)	(1.07,7.88)	(1.18,8.54)
2150	SSP1-2.6	0.01	1.1	2.5	2.6
		(-0.08,0.19)	(0.11,1.89)	(0.67,5.55)	(0.31,6.3)
	SSP5-8.5	0.09	4.50	7.33	8.70
		(-0.05,0.28)	(1.74,7.72)	(1.84,13.45)	(1.74,17.03)
2200	SSP1-2.6	0.03	1.14	2.20	2.50
		(-0.11,0.3)	(-0.14,3.75)	(0.38,4.85)	(-0.03,5.94)
	SSP5-8.5	0.38	5.91	10.48	12.44
		(0.18,0.73)	(2.38,9.96)	(3.54,19.36)	(4.36,26.15)
2250	SSP1-2.6	0.05	1.33	2.49	2.76
		(-0.13,0.4)	(0.01,3.43)	(0.45,5.14)	(0.08,5.82)
	SSP5-8.5	0.93	7.16	14.20	17.57
		(0.4,1.48)	(2.42,12.46)	(3.21,27.20)	(3.92,36.43)
2300	SSP1-2.6	0.07	1.30	2.56	2.66
		(-0.17,0.51)	(-0.14,4.10)	(0.26,5.67)	(-0.21,5.98)
	SSP5-8.5	1.82	7.97	16.04	19.51
		(0.74,3.09)	(3.27,13.79)	(5.88,31.67)	(7.52,40.77)

3.3 Threshold behavior in response to changing climatic boundary conditions

390 The Antarctic Ice Sheet has been shown to exhibit a nonlinear response to warming and hysteresis behavior in quasi–equilibrium (that is, when temperatures change much slower than typical rates of change of an ice sheet; Garbe et al., 2020). In the following, we explore the relationship between climate boundary conditions potentially reached throughout the next centuries and sustained for several thousands of years and the configurations that the Antarctic Ice Sheet evolves to under these conditions

https://doi.org/10.5194/tc-2023-156
Preprint. Discussion started: 9 October 2023

on multi–millennial timescales. These ice–sheet states complement the quasi–equilibrium response of the Antarctic Ice Sheet (obtained by Garbe et al., 2020) as they record the long–term response to faster warming as projected under the different SSP scenarios. Figure 4 shows the committed sea–level contribution of the Antarctic Ice Sheet (in the year 7000) for a given regional (Antarctic–averaged) atmospheric warming level, thereby overcoming the dependency of ice loss on the diverging climate trajectories (Sect. 3.2).

For **regional warming levels of up to 4°C**, as reached by 2300 under SSP1-2.6 and by 2050 under SSP5-8.5, we find a committed collapse of the Amundsen Sea basin, in some cases even a partial collapse of the West Antarctic Ice Sheet, resulting in a long–term Antarctic mass loss of up to 6.0 m sea–level equivalent over multi–millennial timescales (Fig. 4a and b, I and II). With both ice–sheet models, our experiments show a strong grounding–line retreat in the Amundsen Sea Embayment for this temperature range (Fig. 4c and d, I and Fig. 5d and g), consistent with previous work (Garbe et al., 2020). This may be accompanied by a connection from Pine Island Glacier to Ronne Ice Shelf, giving rise to ice loss from this region (Fig. 4c and d, I and Fig. 5a). While Ross Ice Shelf is maintained in simulations with Kori-ULB, it is lost in most simulations with PISM (compare Fig. 4c and d, I). The collapse of Ross Ice Shelf is accompanied by the drainage of the corresponding catchment area (Fig. 4c, I and Fig. 5e and h), except for regional atmospheric warming below 1°C (projected by MRI-ESM2-0 under SSP1-2.6 until year 2050 only) which is comparable with the ice–sheet equilibrium response determined by means of PISM in Garbe et al. (2020). While 2% of the initial ice mass in Antarctica contributing to global mean sea–level rise is lost in Kori-ULB (raising global mean sea–level by up to approximately +2.0 m), a slightly higher fraction of 6% (equivalent to a global mean sea–level change between +3.0 m and +4.0 m) is found in simulations with PISM (Fig. 4b), due to the discharge of larger parts of the West Antarctic Ice Sheet as opposed to an advance of the grounding line in the Siple Coast area in Kori-ULB (compare Fig. 4c and d, I). The uncertainty in the initial ice–sheet configurations of each model results in differences on the order of decimeters in sea–level contribution in this warming range and is thus less significant than the inter–model spread. Overall, there is a good agreement also in the patterns of mass loss for the different initial configurations.

Some of our simulations (across both ice–sheet models) also show an onset of grounding–line retreat in Wilkes basin in this range of atmospheric warming, shifting the upper bound of ice loss up to +6.0 m sea–level equivalent and widening the intra–model spread (Fig. 4b–d, I and Fig. 5i). This region contributes up to +1.5 m to the long–term sea–level change, which may occur for a mean ocean–temperature change exceeding +0.5°C – +1°C in this basin (depending on the ice–sheet model, with earlier onset of retreat in Kori-ULB; Fig. 5i). The loss of ice grounded below sea level in this particular (Wilkes) basin is triggered for slightly lower ocean warming than in Garbe et al. (2020) and Golledge et al. (2015), but is located within the range of idealized experiments by Mengel and Levermann (2014).

The long–term response of the marine basins may further depend on the ratio of atmospheric to oceanic warming: Despite exposing the ice sheet to higher atmospheric warming levels as derived from CESM2–WACCM under the lower–emission pathway, the grounding line in Wilkes subglacial basin does not experience retreat under these forcing conditions (due to weaker ocean forcing compared to UKESM1-0-LL, Fig. 4c, II and Fig. 5i) in PISM experiments. While showing some limited grounding–line retreat in the Wilkes subglacial basin, the sea–level contribution of approximately 1.0 m determined by Kori-ULB is lower due to limited grounding–line retreat and subsequent ice loss in the basins draining Ross Ice Shelf as well as

https://doi.org/10.5194/tc-2023-156
Preprint. Discussion started: 9 October 2023

less pronounced thinning in Recovery basin (compared to PISM; Fig. 4d, II). Exceeding the regional atmospheric warming of 2.5°C projected by CESM2–WACCM under SSP1-2.6 also induces the long–term loss of Filchner–Ronne Ice Shelf in addition to Ross Ice Shelf in PISM experiments (comparable to the long–term response found in Golledge et al. (2015) after following emission pathway RCP4.5 with warming of about 2.2°C), which is accompanied by a retreat of the grounding line in Robin subglacial basin (Fig. 4b and c, II). Ice streams that drain the Recovery basin start showing a contribution to the long–term sea–level change (of about 5.0 m of sea–level equivalent in total for 2.5 °C to 4.0°C of Antarctic–averaged warming) (Fig. 4c, II), which further raises with enhanced warming (Fig. 5c). Such a retreat of the basins connected to Filchner–Ronne Ice Shelf occurs in Kori-ULB only at slightly higher warming levels (see below, Fig. 4d).

Antarctic atmospheric warming levels of +5°C to +7°C are projected by the end of this century when following the higher–emission pathway (Fig. 4 III). Under such climatic boundary conditions, the ice–sheet decline continues on the long–term in regions which are already affected by lower warming levels, resulting in an ice loss of between +1.2 m and +8.5 m sea–level equivalent (Fig. 4a, III). This wide spread contains the recent estimate by Van Breedam et al. (2020) of +6.6 m sea–level equivalent under warming of approximately +7°C over the next 10 000 years. In this warming range, ice loss from the Ross Ice Shelf catchment in West Antarctica substantially contributes to sea–level change also in Kori-ULB (Fig. 4d, III and Fig. 5e and h). That is, we find a complete collapse of the West Antarctic Ice Sheet in both ice–sheet models for an Antarctic–averaged atmospheric warming above +4°C. The inter–model spread in mass loss is explained by a stronger thinning of ice draining into the eastern Weddell Sea region in PISM in combination with a more pronounced thickening in the inner parts of East Antarctica in Kori-ULB within this warming range (compare Fig. S16–S17 for Kori-ULB with Fig. S18–S19 for PISM when sustaining warming projected for year 2100).

Exceeding an **atmospheric warming of +8°C in Antarctica** gives rise to a further increase in the fraction of ice that is lost on multi–millennial timescales from 15 % up to 40 % at +14°C (Fig. 4 IV). Enhanced long–term mass loss with stronger Antarctic warming is found in particular for Filchner–Ronne, Recovery and Wilkes subglacial basins (Fig. 5a–c, i). In addition, some of our experiments suggest the onset of ice drainage from the East Antarctic Aurora basin (Fig. 5f; in accordance with Golledge et al., 2015), associated with a substantially increasing contribution to sea–level rise from this basin (for RACMO initial state, Fig. S19) in this warming range. The ice stored in the Aurora basin is lost completely in both ice–sheet models for even higher atmospheric warming levels (see below and Fig. 4V). While the general dependency of ice loss from the Aurora region on the atmospheric forcing in our simulations is in agreement with Golledge et al. (2017), stronger warming of the atmosphere is required here for triggering the retreat.

For sustained **regional atmospheric warming above +15°C** (projected by CESM2–WACCM after year 2200), we find that large parts of the marine basins in Antarctica are lost and ice grounded above sea level in East Antarctica starts to decline substantially on multi–millennial timescales (Fig. 4V). Over the next millennia, this gives rise to an ice loss equivalent to a sea–level change of up to +40.8 m. It cannot be ruled out that Antarctica could become ice–free under the given climate conditions, consistent with Garbe et al. (2020) and Winkelmann et al. (2015), given the continued increase of the Antarctic sea–level contribution at the end of our simulations (Fig. 2d).

https://doi.org/10.5194/tc-2023-156
Preprint. Discussion started: 9 October 2023

The Cryosphere Discussions
Open Access
EGU

Overall, the sea–level commitment increases nonlinearly with increasing atmospheric temperature change in Antarctica (Fig. 4a), with a spread in mass loss at a given warming level due to differences in parameter choices (here arising as part of the initialisation) and structural (model) uncertainty. In other words, the ice–sheet sensitivity to warming varies with the initial Antarctic ice–sheet configuration and its characteristics. While we can identify distinct clusters of qualitatively different ice–sheet behavior on the continental–scale with changing atmospheric warming (Fig. 4), critical thresholds in climatic boundary conditions inducing persistent ice loss are masked in the continent–wide committed sea–level contribution and can be located on a basin–scale (Fig. 5). The importance of structural differences between the ice–sheet models, their initialisation and related parameter choices for Antarctic sea–level commitment and respective critical temperature thresholds is discussed in Sect. 4.1.

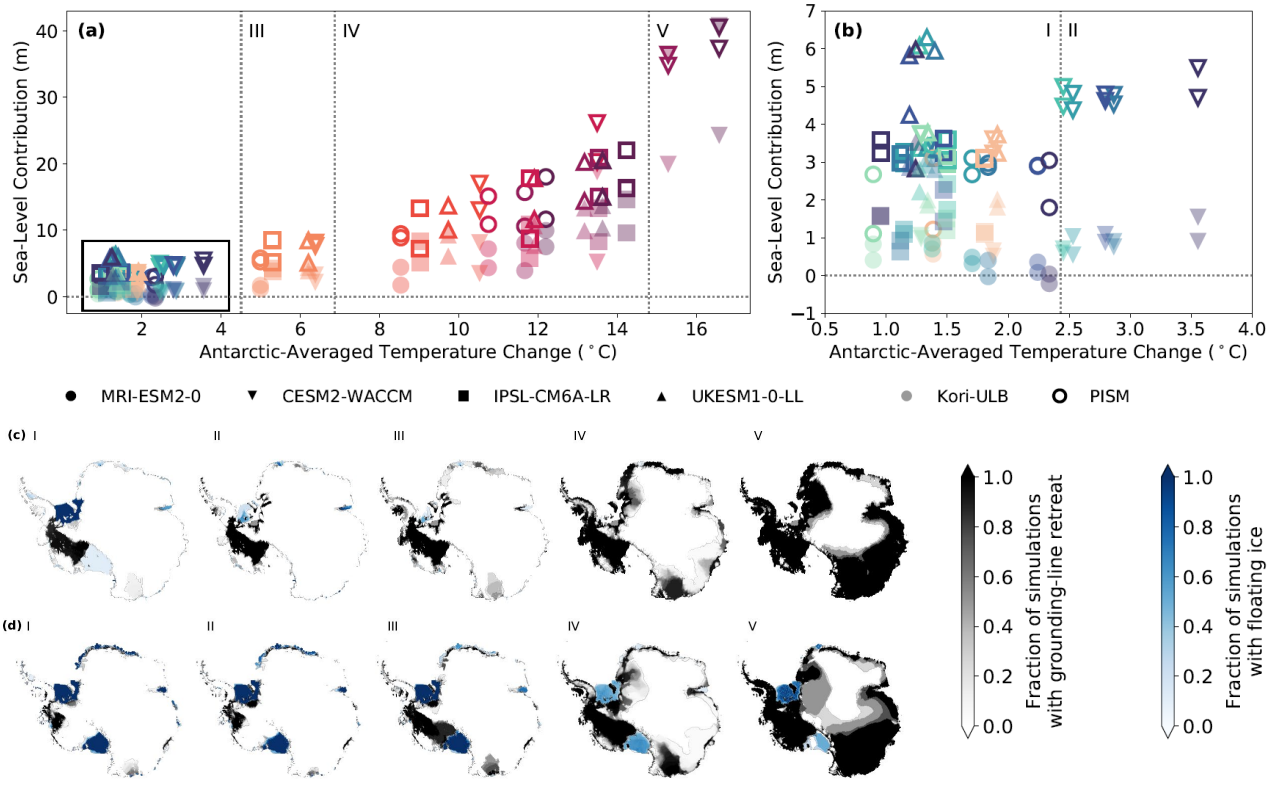

Figure 4. Committed sea–level contribution from the Antarctic Ice Sheet. (a) and (b): Long–term ice loss from the Antarctic Ice Sheet (in meters sea–level equivalent) for year 7000 in response to Antarctic–averaged atmospheric temperature change (compared to 1995–2014). The change in climatic boundary conditions is sustained for several millennia. (b) is a zoom into (a) for a lower atmospheric temperature change. (c) and (d): Fractions of experiments that show grounding–line retreat in year 7000 in PISM and Kori-ULB, respectively. The fraction is determined for all experiments that are assigned to the distinct clusters I–V.

https://doi.org/10.5194/tc-2023-156
Preprint. Discussion started: 9 October 2023

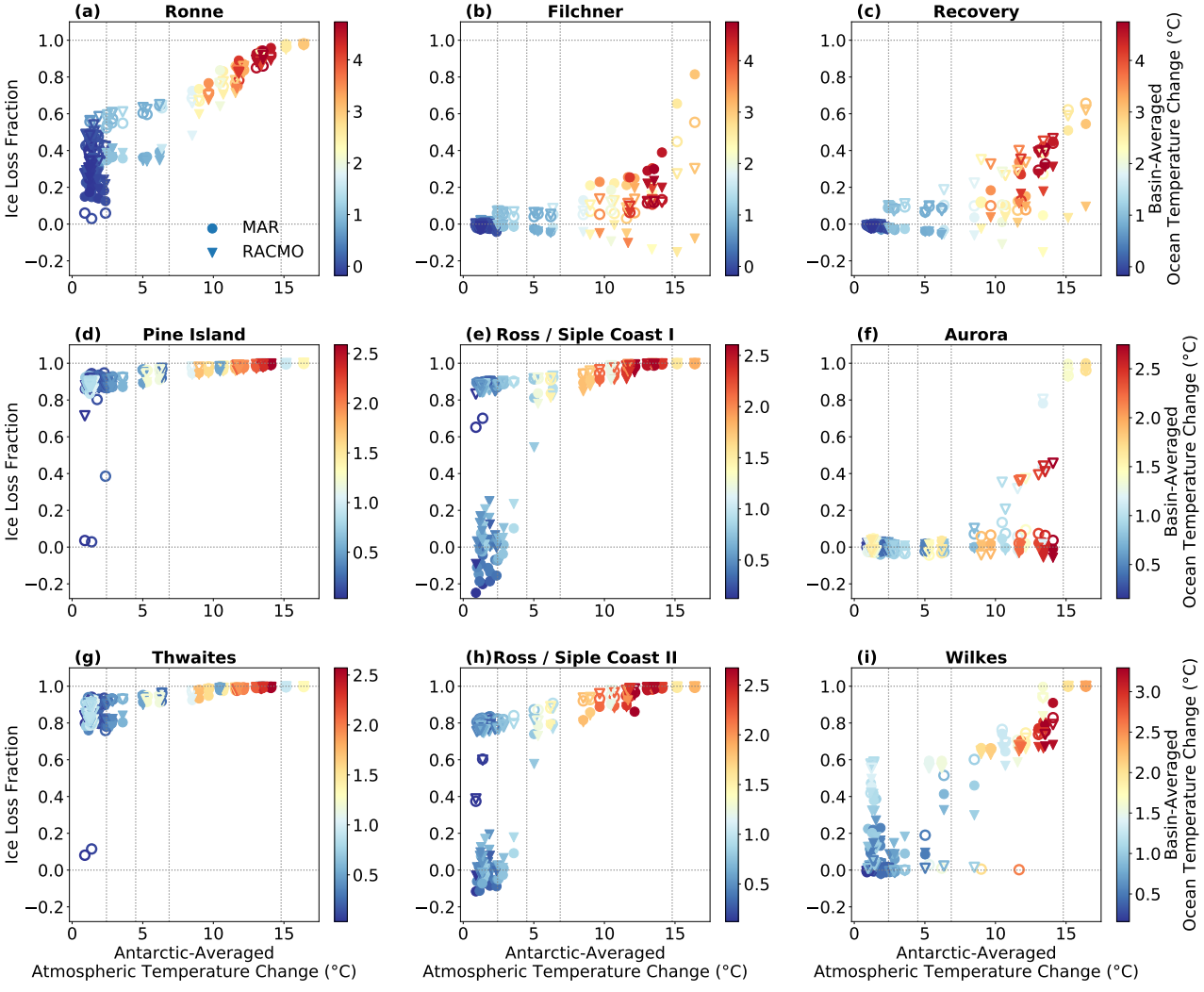

Figure 5. Ice loss from Antarctic drainage basins. Long–term ice loss from different Antarctic drainage basins (as fraction of respective sea–level rise potential) for the year 7000 in response to Antarctic–averaged atmospheric temperature change (compared to 1995–2014). The basin–averaged oceanic temperature change is represented by the colouring. Open and filled markers correspond to the long–term ice loss determined by PISM and Kori-ULB, respectively.

https://doi.org/10.5194/tc-2023-156
Preprint. Discussion started: 9 October 2023

4 Discussion

In this paper, we determine the multi–millennial sea–level contribution from mass balance changes of the Antarctic Ice Sheet under a range of possible climate trajectories for both low– and high–emission pathways. In particular, we quantify the long–term Antarctic sea–level commitment when stabilising climatic boundary conditions at different points in time. That is, the atmospheric and oceanic changes potentially established during the upcoming centuries are sustained for several thousands of years, and we explore their long–term impacts on the Antarctic Ice Sheet. Experiments were carried out systematically for stabilized climate at different points in time over the course of the next centuries and in a consistent way with the stand–alone ice–sheet models PISM and Kori-ULB accounting for some inter– and intra–model uncertainty.

Our experiments illustrate a substantial gap between the *realized* and *committed* sea–level change from the Antarctic Ice Sheet. While the projected Antarctic mass change by the end of this century may raise global mean sea–level by a few centimeters (or could potentially result in a sea–level drop, spanning a range from -0.1 m to +0.1 m sea–level equivalent), the Antarctic Ice Sheet may be committed to a strong grounding–line retreat in the Amundsen Sea Embayment up to a collapse of the West Antarctic Ice Sheet for sustained climate conditions at levels projected to be reached during this century (that is, branching off in the years 2050 or 2100, depending on the GCM) even under the lower–emission pathway. Mass loss from the marine Wilkes subglacial basin in East Antarctica may unfold on multi–millennial timescales for warm ocean conditions projected by some GCMs as early as the second half of this century under the lower–emission scenario. Stabilizing climate conditions later in time (for instance in the year 2300) and following the higher–emission pathway SSP5-8.5 may additionally trigger a substantial decline of the terrestrial East Antarctic Ice Sheet, resulting in long–term mass losses of up to +40.8 m sea–level equivalent.

Determining the committed evolution of the Antarctic Ice Sheet triggered by the warming projected for the next centuries extends previous studies of the long–term ice–sheet response (especially in the Amundsen Sea sector) under sustained present–day conditions. For example, Reese et al. (2023) and Golledge et al. (2019) suggest a committed (potentially irreversible) grounding–line retreat in West Antarctica under present–day conditions on centennial timescales in response to atmospheric and oceanic changes over the past decades. We also add to the assessment of the long–term Antarctic sea–level commitment to future warming by the end of this century (Chambers et al., 2022; Lowry et al., 2021) and by 2300 (Golledge et al., 2015; Bulthuis et al., 2019; Coulon et al., 2023) by exploring the multi–millennial consequences of stabilizing climatic boundary conditions at different points in time over the course of the next centuries, in a consistent way for two ice–sheet models. From a dynamical systems perspective, the long–term stability of the Antarctic Ice Sheet under present and potential future rates of warming (being much faster than typical rates of change in an ice sheet) is studied. This complements the quasi–equilibrium ice–sheet response to warming presented by Garbe et al. (2020) and, thereby, bridges the gap to the transient realized sea–level change from Antarctica (e.g., by the end of this century as in Seroussi et al., 2020).

https://doi.org/10.5194/tc-2023-156
Preprint. Discussion started: 9 October 2023

4.1 Uncertainties in Antarctic sea–level commitment

The committed Antarctic sea–level contribution is subject to uncertainties related to the substantial spread of warming projected by the selected GCMs for a given point in time (*climate forcing uncertainty*, Sect. 3.2). Critical temperature thresholds giving rise to self–sustained ice loss further vary in our experiments as a result of *inter–* and *intra–model uncertainties* (Sect. 3.3). These uncertainties may be induced by differences in the model structure and the parameterisation of certain processes (e.g., Seroussi et al., 2020), initialisation procedures (e.g., Seroussi et al., 2019; Aðalgeirsdóttir et al., 2014) as well as parameter choices (e.g., Bulthuis et al., 2019; Nias et al., 2016; Coulon et al., 2023). The role of these different sources of uncertainties for the multi–millennial Antarctic sea–level response presented in this work is discussed in the following.

Uncertainty due to climate forcing

The climate forcing from the four GCMs employed here results in a wide spread of the realized and especially committed sea–level contribution from Antarctica, making it one of the most important sources of uncertainty.

For low to intermediate warming levels covered by the lower–emission pathway SSP1-2.6, the uncertainty introduced by the climate forcing at a given point in time is comparable to the uncertainty caused by inter–model differences (compare Fig. 2e), except for the response to CESM2–WACCM under SSP1-2.6. Here, PISM shows an onset of ice discharge from the Recovery basin after Filchner–Ronne Ice Shelf is lost (Fig. S14–15), while corresponding ice loss is triggered for stronger changes in climatic boundary conditions in Kori-ULB (compare Fig. S12–S13 for SSP1-2.6 to Fig. S16–S17 for SSP5-8.5). This gives rise to a larger difference in the Antarctic sea–level contribution determined by both ice–sheet models.

We find that the growing spread of the committed Antarctic sea–level contribution under the higher–emission scenario SSP5-8.5 for stabilizing the ice–sheet boundary conditions later in time can (to a large part) be attributed to the divergence of the climate trajectories projected by the four GCMs. They are characterized by different warming rates and climate sensitivities, resulting in a substantial climate forcing uncertainty at a specific point in time: While for MRI-ESM2-0 a comparably low equilibrium climate sensitivity was determined (3.2°C, below the multimodel mean of 3.7°C; Meehl et al., 2020), the equilibrium climate sensitivities of UKESM1-0-LL (5.3°C), CESM2-WACCM (4.8°C) and IPSL-CM6A-LR (4.6°C) are at the upper end of the range of climate sensitivities reported for CMIP6. CESM2-WACCM also shows a significantly stronger regional atmospheric warming under SSP5-8.5 beyond 2150 than the other GCMs (Tab. S1). This translates into a growing uncertainty in projected long–term Antarctic ice loss under SSP5-8.5 with a substantially higher committed sea–level contribution from Antarctica for the same year under CESM2-WACCM compared to the other applied CMIP6 GCMs. For example, the committed Antarctic sea–level contribution determined by Kori-ULB and PISM under CESM2-WACCM ranges between 24.3 m and 40.8 m (when assuming a stabilization of climatic conditions representative for the year 2300). In contrast, we find an Antarctic mass loss of up to 22.0 m for the other CMIP6 GCMs.

https://doi.org/10.5194/tc-2023-156
Preprint. Discussion started: 9 October 2023

Uncertainty arising from intra– and inter–model differences

On multi–millennial timescales, both ice–sheet models show a good agreement in the pattern of mass loss and the resulting sea–level contribution from Antarctica for strong atmospheric warming (above 15°C of regional atmospheric temperature change), where the ice–sheet's decline (predominantly of its terrestrial parts grounded above sea level) is driven by atmospheric changes rather than ocean warming. The onset of grounding–line retreat in Antarctic marine basins is located at different low to intermediate warming levels due to *inter–model differences*. Both ice–sheet models agree on an early retreat of grounding lines of Pine Island and Thwaites Glacier in the Amundsen Sea Embayment, consistent with previous findings that the grounding–lines may at present already be undergoing a self–sustained retreat or that this retreat has been locked in due to changes in the climatic boundary conditions over the past decades (Favier et al., 2014; Golledge et al., 2019; Reese et al., 2023). Ice loss from the catchment draining Ross Ice Shelf and a (partial) collapse of the West Antarctic Ice Sheet is triggered, however, for lower warming in PISM than in Kori-ULB, resulting in a multi–meter spread of the long–term committed sea–level contribution for Antarctic–averaged atmospheric warming up to 4°C (Fig. 4). This grounded ice–sheet response is accompanied by a different response of the major ice shelves in both ice–sheet models. Sequential collapse of the Ross and Filchner–Ronne Ice Shelf is projected by PISM for the change in oceanic and atmospheric conditions projected under SSP1-2.6, while both shelves are preserved in Kori-ULB under this lower–emission pathway and in some cases even under the higher–emission pathway SSP5-8.5. Ice–sheet sensitivities of the marine Wilkes and Recovery subglacial basins in East Antarctica to changes in atmospheric and oceanic boundary conditions also vary depending on the ice–sheet model configuration, such that persistent ice loss is triggered for different magnitudes of warming.

This inter–model discrepancy may be the result of several factors related to the characteristics of both ice–sheet models: The grounding line in the Siple Coast area is relatively sensitive to changes in climatic boundary conditions in PISM, being located upstream of the observed grounding line at present–day (compare Fig. S1; as often observed in a model initialisation in a spin–up approach, e.g., Reese et al., 2023) and showing thinning in Ross Ice Shelf over the historical period (compare Fig. S2; also when determining the historical ice–sheet evolution on higher horizontal resolution using PISM,e.g., Reese et al., 2020, 2023). The grounding–line advance in the Siple Coast found in Kori-ULB under SSP1-2.6 may result from a drift of the initialisation procedure, which could be due to an underestimation of the sub–shelf melt rates obtained from PICO compared to the balance melt rates derived during the nudging procedure (Sect. 2.2.2). Finally, some ice shelves are sustained longer in Kori-ULB, which could be due to the different calving schemes employed in the ice–sheet models (Levermann et al., 2012; Pollard et al., 2015; DeConto and Pollard, 2016).

Our simulations are performed on a comparably coarse horizontal resolution of 16 km, allowing for a large number of experiments as presented here, which is needed to cover the wide range of uncertainties. The migration of the grounding line in PISM is captured reasonably well, even on such a coarse resolution, with a sub–grid interpolation scheme (Feldmann et al., 2014), which allows to reproduce glacial cycles of the Antarctic Ice Sheet (Albrecht et al., 2020). Garbe et al. (2020) showed (using PISM) that the overall hysteresis behavior of the Antarctic Ice Sheet is robust across model resolution. In Kori-ULB,

https://doi.org/10.5194/tc-2023-156
Preprint. Discussion started: 9 October 2023

565 resolving grounding–line dynamics at a coarse resolution is addressed by imposing a flux condition (Pollard and DeConto, 2012a, 2020), which results in a good agreement with high–resolution models.

Characteristics of the initial states give rise to an *intra–model* spread in the projected multi–millennial sea–level contribution for a given warming level. In our experiments, we rely on two different present–day atmospheric climatologies (Kittel et al., 2021; Van Wessem et al., 2018) that are involved in building the respective initial ice–sheet configurations (Sect. 2.2.2). 570 While a recent intercomparison concluded that Antarctic climate is represented reasonably well compared to observations in state–of–the–art RCMs, disagreement with respect to precipitation and atmospheric temperatures between the RCMs still exists for some areas (Mottram et al., 2021). For enhanced atmospheric warming, the difference between the initial states of Kori-ULB constructed with the atmospheric climatologies derived from MAR and RACMO increases in terms of sea–level contribution. For warming covered by the lower–emission pathway SSP1-2.6, the difference on the order of decimeters of sea– 575 level equivalent (Fig. S20) is due to varying ice–sheet sensitivities of both initial states in the Wilkes suglacial basin and the Siple Coast (Fig. S12–S13). The gap in mass loss amounts to multiple meters of sea–level equivalent for an Antarctic–averaged atmospheric warming above 15°C (compare Fig. S20). Most of the marine–based portions of Antarctica are lost already before reaching this warming range, such that this difference arises from a stronger decline of ice grounded above sea level for the atmospheric climatology derived from MAR than from RACMO, potentially caused by enhanced surface melting with the 580 former. The initial states built in a spin–up approach with PISM differ in their dynamical response due to the distinct parameter combinations favoured by the scoring in the initial–state ensembles for the distinct atmospheric climatologies (Reese et al., 2023; Albrecht et al., 2020, see Sect. 2.2.2). Overall, we find that mass loss is higher for the RACMO initial state with a lower pseudo–plastic sliding exponent $q = 0.5$ (compared to $q = 0.75$ as an outcome of the initialisation given the MAR atmospheric climatology, comparable with Lowry et al., 2021). This is the case both during the historical period and for a large range 585 of the covered projected atmospheric temperature changes (Fig. S20). For a regional atmospheric warming of up to about 4°C the difference in sea–level contribution between the PISM initial states is generally on the order of decimeters. Given an initialisation with the atmospheric climatology derived from RACMO, the ice sheet is more sensitive to changes in its climatic boundary conditions in the Recovery and Aurora basin (occurring for Antarctic–averaged atmospheric temperature changes above approximately +8°C), with a global mean sea–level change being up to +9.0 m higher compared to the MAR initial state. 590 The response of both present–day representations of Antarctica to strong regional warming above +15°C (where the decline of remaining terrestrial parts in East Antarctica dominates) agrees well. Here, a slightly more pronounced mass loss is found for the ice–sheet initialisation involving the MAR atmospheric climatology (with higher atmospheric temperatures enhancing surface melt and runoff of the remaining ice grounded above sea level).

While taking into account distinct Antarctic ice–sheet representations as a result of an initial–state ensemble covering rel- 595 evant model parameters, some sources of intra–model uncertainties cannot be further explored here due to computational constraints in favor of sampling a wide range of possible future climates. One of these is the uncertainty related to the sub–shelf melt parameterisation: To determine sub–shelf melt, PICO (Reese et al., 2018) with a fixed combination of the overturning parameter and the effective turbulent heat exchange coefficient parameter is chosen out of a diverse set of available sub–shelf melt parameterisations (recently compared in Burgard et al., 2022). PICO has been shown to reproduce observed basal melt

https://doi.org/10.5194/tc-2023-156
Preprint. Discussion started: 9 October 2023

rates averaged over Antarctic ice shelves related to the vertical overturning circulation in ice–shelf cavities and to resemble the typical pattern of strongest melt near the grounding line (Reese et al., 2018, 2023). However, smoother spatial fields of basal melt in PICO compared to observations (Reese et al., 2018) and determining melt as linearly related to temperature (Reese et al., 2018; Burgard et al., 2022) may eventually impact long–term ice dynamics. In a next step, the long–term ice–sheet response when including larger parts of the parameter space covered in the initial–state ensemble and beyond could be explored, allowing to quantify how parametric uncertainty translates into multi–millennial Antarctic sea–level commitment.

4.2 Limitations in assessing Antarctic sea–level commitment

Boundary conditions

Following recent efforts in projecting the Antarctic sea–level contribution on different timescales ranging from the next decades until 2100 to several millennia (Seroussi et al., 2020; Payne et al., 2021; Golledge et al., 2019, 2015), we base the imposed changes in climatic conditions in Antarctica on state–of–the–art GCMs from the Coupled Model Intercomparison Project CMIP6. Biases in the chosen GCMs and a poor representation of conditions at the ice–sheet margins due to their coarse resolution (Beadling et al., 2020; Bracegirdle et al., 2020; Purich and England, 2021) may influence the simulated mass changes of the Antarctic Ice Sheet presented here. First of all, this is relevant for interpreting the simulated historic evolution of the ice sheet because it captures the response to the changes in atmospheric and oceanic conditions over the past decades simulated by one selected GCM (NorESM1-M; Barthel et al., 2020; Bentsen et al., 2013) only. Including the historic ice–sheet trajectory was shown to be essential for Antarctic sea–level projections by 2100 (Reese et al., 2020). Potential biases in the historic ice–sheet evolution (due to biases in the forcing, but likewise in the ice–sheet models itself) may also play a role for the multi–millennial ice–sheet response presented here. The GCMs available to provide future changes in boundary conditions until 2300 are characterized by a large range of climate sensitivities with a high upper bound (Meehl et al., 2020), which has been suggested to not be in accordance with paleoclimate evidence (Zhu et al., 2021). It introduces large uncertainties in the Antarctic sea–level commitment for fixing climatic boundary conditions at the same point in time (as discussed above). Consequently, the derived future climate trajectories and respective projected multi–millennial Antarctic ice loss should only be related to emissions with care and can rather be seen as a potential range of climate futures for Antarctica.

For determining the long–term Antarctic sea–level commitment, we assume constant climate conditions on multi–millennial timescales. Keeping climatic boundary conditions constant on multi–millennial timescales allows us to assess the long–term ice–sheet stability and committed sea–level contribution under an idealized combination of atmospheric and oceanic changes with respect to present–day. This approach has been invoked previously (e.g., Golledge et al., 2015), but comes with certain assumptions: For instance, a continued ocean response to changing CO_2 conditions and atmospheric warming (Li et al., 2013) may result in an altered ratio of atmospheric and oceanic changes beyond the point in time where a stabilization of climatic boundary conditions is assumed here. In addition, observed interannual and decadal variability (Paolo et al., 2018; Jenkins et al., 2018) is neglected in the imposed constant climate conditions for simplicity, which has been shown to potentially result

https://doi.org/10.5194/tc-2023-156
Preprint. Discussion started: 9 October 2023

in a lower long–term ice–sheet volume (compared to a stable climate; Mikkelsen et al., 2018) up to ice–sheet retreat (Christian et al., 2020; Robel et al., 2019).

Finally, climate trajectories distinct from climate stabilization scenarios may impact the Antarctic Ice Sheet response in the near and far future. This includes increasingly discussed (temperature) overshoot pathways showing a reversal of climate conditions after exceeding a warming of, e.g., 1.5°C (Tokarska et al., 2019). The corresponding response of the Antarctic Ice Sheet is, however, not well constrained. In particular, the timescale difference between the ice sheet's response and the potentially high rates of future warming may allow for trajectories deviating from the equilibrium response of the ice sheet. That is, large–scale ice–sheet changes described here may potentially be reversible despite having crossed a critical threshold upon reverting temperatures to present-day or pre–industrial climate conditions in a 'safe' overshoot (Ritchie et al., 2021). Our experiments form the basis for assessing the response of the Antarctic Ice Sheet to a reversal of climatic boundary conditions and relevant timescales. It will allow us to characterize the (ir-)reversibility of the Antarctic mass loss presented here.

Missing feedback mechanisms relevant for long–term Antarctic mass loss

Several positive and negative feedbacks (Fyke et al., 2018) between the Antarctic Ice Sheet and the Earth system are missing in stand–alone ice–sheet model projections such as the ones presented here, but may be relevant for the long–term stability of the Antarctic Ice Sheet. Including the missing feedbacks in future fully–coupled assessments of the Antarctic sea–level commitment could change the timing and rates of (abrupt) mass loss determined in our experiments, either by dampening or by accelerating Antarctic ice loss. However, such fully–coupled Earth system models including the ice sheets, which are capable of simulating the multi–millennial response as needed for this study, are not yet available. We here include some of the relevant feedbacks using parametrisations: Atmospheric temperature imposed to the Antarctic Ice Sheet is modified in our experiments using the atmospheric lapse rate to account for the impact of a changing ice–surface elevation. This also feeds into the surface melt determined by the positive–degree–day approach, depicting the surface melt–elevation feedback (Levermann and Winkelmann, 2016). The potentially strong decline of ice volume under warming projected for higher–emission pathways may, however, additionally result in changes of the atmospheric circulation and respective precipitation patterns (compare e.g., Merz et al., 2014, for Greenland), which are not covered in our experiments. By applying the positive–degree–day approach to determine the future ice–sheet surface melt, we do not account for the self–amplifying melt–albedo feedback (Jakobs et al., 2019, 2021). While polar–oriented regional climate models cannot provide boundary conditions (or dynamically interact with ice sheets) on multi–millennial timescales considered here as of yet, approaches of intermediate complexity such as the recently introduced (simple) diurnal Energy Balance Model (Garbe et al., 2023; Zeitz et al., 2021) may allow to include the potentially accelerating effect of changes in albedo on projected ice loss through enhanced surface melting (Garbe et al., 2023) in the future. In addition, freshwater fluxes from mass balance changes of the Antarctic Ice Sheet into the surrounding ocean have been suggested to result in atmospheric cooling in the Southern Hemisphere competing with a potential enhancement of ice loss by the end of the century in a positive feedback due to subsurface ocean warming (Golledge et al., 2019). This self–amplifying feedback could have played a role in abrupt ice discharge events during the last deglaciation (Weber et al., 2014). It remains to be explored how such ice–ocean feedbacks could play out on multi–millennial timescales in Antarctica's future.

https://doi.org/10.5194/tc-2023-156
Preprint. Discussion started: 9 October 2023

Finally, while bedrock adjustment to changes in ice load is included in our experiments, opposing Earth structures between West and East Antarctica are not considered: By assuming uniform solid–Earth properties, ocean–driven ice loss from marine basins in East Antarctica may be underestimated on millennial timescales (Coulon et al., 2021), such that our estimates of committed East Antarctic mass loss may be seen as conservative. On the other hand, taking into account characteristic rheological properties of the solid Earth in West Antarctica could promote rapid bedrock uplift, thereby delaying ice–sheet changes.

While various sources of uncertainties remain to be explored for quantifying the long–term Antarctic sea–level commitment, our analysis shows (across distinct ice–sheet models) that the long–term multi–millennial impacts on the Antarctic Ice Sheet of warming projected for a given point in time are profound when compared to the sea–level change realized at this point in time. Our findings thus stress the importance of complementing typical decadal–to–centennial projections of the future evolution of the Antarctic Ice Sheet by the respective committed Antarctic sea–level contribution for long–term decision making.

Code and data availability. The source code of PISM is publicly available on GitHub via https://www.pism.io. The exact PISM version used in this paper will be archived within the open access repository Zenodo upon publication of the manuscript. The code of the Kori-ULB ice–sheet model is publicly available on GitHub via https://github.com/FrankPat/Kori-dev. All datasets used in this study are freely accessible through their original references. The CMIP6 forcing data used in this study are accessible through the CMIP6 search interface (https://esgf-node.llnl.gov/search/cmip6/). The simulations outputs, the data needed to produce the figures and tables, and the scripts will be hosted on Zenodo upon publication of the final paper.

Author contributions. R.W. conceived the study. A.K.K. and V.C. processed the forcing data, initialized the ice–sheet models and ran the model simulations. A.K.K. performed the data analysis, produced the figures and wrote the original manuscript with regular inputs from V.C. All authors contributed to the final version of the manuscript.

Competing interests. The authors declare that they have no conflict of interest.

Acknowledgements. This project has received funding from the European Union's Horizon 2020 research and innovation programme under grant agreement No. 869304 (PROTECT). The authors gratefully acknowledge the European Regional Development Fund (ERDF), the German Federal Ministry of Education and Research (BMBF) and the Land Brandenburg for supporting this project by providing resources on the high-performance computer system at the Potsdam Institute for Climate Impact Research. Development of PISM is supported by NASA grants 20-CRYO2020-0052 and 80NSSC22K0274 and NSF grant OAC-2118285. Computational resources for Kori-ULB simulations have been provided by the Consortium des Équipements de Calcul Intensif (CÉCI), funded by the Fonds de la Recherche Scientifique de Belgique (F.R.S.-FNRS) under Grant No. 2.5020.11 and by the Walloon Region. A.K.K. and R.W. further acknowledge support by the

https://doi.org/10.5194/tc-2023-156
Preprint. Discussion started: 9 October 2023

European Union's Horizon 2020 research and innovation programme under Grant Agreement No. 820575 (TiPACCs). We acknowledge the
695 World Climate Research Programme's Working Group on Coupled Modelling, which is responsible for CMIP, and we thank the climate modelling groups (whose models are listed in Table S1 of this paper) for producing and making their model output available. This work has been performed in the context of the FutureLab on Earth Resilience in the Anthropocene at the Potsdam Institute for Climate Impact Research.

https://doi.org/10.5194/tc-2023-156
Preprint. Discussion started: 9 October 2023

References

Aðalgeirsdóttir, G., Aschwanden, A., Khroulev, C., Boberg, F., Mottram, R., Lucas-Picher, P., and Christensen, J.: Role of model initialization for projections of 21st-century Greenland ice sheet mass loss, Journal of Glaciology, 60, 782–794, https://doi.org/10.3189/2014JoG13J202, 2014.

Adusumilli, S., Fricker, H. A., Medley, B., Padman, L., and Siegfried, M. R.: Interannual variations in meltwater input to the Southern Ocean from Antarctic ice shelves, Nature Geoscience, 13, 616–620, https://doi.org/10.1038/s41561-020-0616-z, 2020.

Aitken, A., Roberts, J., Van Ommen, T., Young, D., Golledge, N., Greenbaum, J., Blankenship, D., and Siegert, M.: Repeated large-scale retreat and advance of Totten Glacier indicated by inland bed erosion, Nature, 533, 385–389, https://doi.org/10.1038/nature17447, 2016.

Albrecht, T., Winkelmann, R., and Levermann, A.: Glacial-cycle simulations of the Antarctic Ice Sheet with the Parallel Ice Sheet Model (PISM) – Part 1: Boundary conditions and climatic forcing, The Cryosphere, 14, 599–632, https://doi.org/10.5194/tc-14-599-2020, 2020.

Armstrong McKay, D. I., Staal, A., Abrams, J. F., Winkelmann, R., Sakschewski, B., Loriani, S., Fetzer, I., Cornell, S. E., Rockström, J., and Lenton, T. M.: Exceeding 1.5° C global warming could trigger multiple climate tipping points, Science, 377, eabn7950, https://doi.org/10.1126/science.abn7950, 2022.

Arthern, R. J. and Williams, C. R.: The sensitivity of West Antarctica to the submarine melting feedback, Geophysical Research Letters, 44, 2352–2359, https://doi.org/10.1002/2017GL072514, 2017.

Barletta, V. R., Bevis, M., Smith, B. E., Wilson, T., Brown, A., Bordoni, A., Willis, M., Khan, S. A., Rovira-Navarro, M., Dalziel, I., et al.: Observed rapid bedrock uplift in Amundsen Sea Embayment promotes ice-sheet stability, Science, 360, 1335–1339, https://doi.org/10.1126/science.aao1447, 2018.

Barthel, A., Agosta, C., Little, C. M., Hattermann, T., Jourdain, N. C., Goelzer, H., Nowicki, S., Seroussi, H., Straneo, F., and Bracegirdle, T. J.: CMIP5 model selection for ISMIP6 ice sheet model forcing: Greenland and Antarctica, The Cryosphere, 14, 855–879, https://doi.org/10.5194/tc-14-855-2020, 2020.

Beadling, R. L., Russell, J., Stouffer, R., Mazloff, M., Talley, L., Goodman, P., Sallée, J.-B., Hewitt, H., Hyder, P., and Pandde, A.: Representation of Southern Ocean properties across coupled model intercomparison project generations: CMIP3 to CMIP6, Journal of Climate, 33, 6555–6581, https://doi.org/10.1175/JCLI-D-19-0970.1, 2020.

Bentsen, M., Bethke, I., Debernard, J. B., Iversen, T., Kirkevåg, A., Seland, Ø., Drange, H., Roelandt, C., Seierstad, I. A., Hoose, C., et al.: The Norwegian Earth System Model, NorESM1-M–Part 1: description and basic evaluation of the physical climate, Geoscientific Model Development, 6, 687–720, https://doi.org/10.5194/gmd-6-687-2013, 2013.

Bernales, J., Rogozhina, I., and Thomas, M.: Melting and freezing under Antarctic ice shelves from a combination of ice-sheet modelling and observations, Journal of Glaciology, 63, 731–744, https://doi.org/10.1017/jog.2017.42, 2017.

Blackburn, T., Edwards, G., Tulaczyk, S., Scudder, M., Piccione, G., Hallet, B., McLean, N., Zachos, J., Cheney, B., and Babbe, J.: Ice retreat in Wilkes Basin of East Antarctica during a warm interglacial, Nature, 583, 554–559, https://doi.org/10.1038/s41586-020-2484-5, 2020.

Bracegirdle, T., Holmes, C., Hosking, J., Marshall, G., Osman, M., Patterson, M., and Rackow, T.: Improvements in circumpolar Southern Hemisphere extratropical atmospheric circulation in CMIP6 compared to CMIP5, Earth and Space Science, 7, e2019EA001 065, https://doi.org/10.1029/2019EA001065, 2020.

Bueler, E. and Brown, J.: Shallow shelf approximation as a "sliding law" in a thermomechanically coupled ice sheet model, Journal of Geophysical Research: Earth Surface, 114, https://doi.org/10.1029/2008JF001179, 2009.

https://doi.org/10.5194/tc-2023-156
Preprint. Discussion started: 9 October 2023

Bueler, E. and van Pelt, W.: Mass–conserving subglacial hydrology in the Parallel Ice Sheet Model version 0.6, Geoscientific Model Development, 8, 1613–1635, https://doi.org/gmd-8-1613-2015, 2015.

Bueler, E., Lingle, C. S., and Brown, J.: Fast computation of a viscoelastic deformable Earth model for ice-sheet simulations, Annals of Glaciology, 46, 97–105, https://doi.org/10.3189/172756407782871567, 2007.

Bulthuis, K., Arnst, M., Sun, S., and Pattyn, F.: Uncertainty quantification of the multi-centennial response of the Antarctic ice sheet to climate change, The Cryosphere, 13, 1349–1380, https://doi.org/10.5194/tc-13-1349-2019, 2019.

Burgard, C., Jourdain, N. C., Reese, R., Jenkins, A., and Mathiot, P.: An assessment of basal melt parameterisations for Antarctic ice shelves, The Cryosphere, 16, 4931–4975, https://doi.org/tc-16-4931-2022, 2022.

Calov, R. and Greve, R.: A semi-analytical solution for the positive degree-day model with stochastic temperature variations, Journal of Glaciology, 51, 173–175, https://doi.org/10.3189/172756505781829601, 2005.

Chambers, C., Greve, R., Obase, T., Saito, F., and Abe-Ouchi, A.: Mass loss of the Antarctic ice sheet until the year 3000 under a sustained late-21st-century climate, Journal of Glaciology, 68, 605–617, https://doi.org/10.1017/jog.2021.124, 2022.

Christian, J. E., Robel, A. A., Proistosescu, C., Roe, G., Koutnik, M., and Christianson, K.: The contrasting response of outlet glaciers to interior and ocean forcing, The Cryosphere, 14, 2515–2535, https://doi.org/10.5194/tc-14-2515-2020, 2020.

Clark, P. U., Shakun, J. D., Marcott, S. A., Mix, A. C., Eby, M., Kulp, S., Levermann, A., Milne, G. A., Pfister, P. L., Santer, B. D., et al.: Consequences of twenty-first-century policy for multi-millennial climate and sea-level change, Nature Climate Change, 6, 360–369, https://doi.org/10.1038/nclimate2923, 2016.

Clarke, G. K., Nitsan, U., and Paterson, W.: Strain heating and creep instability in glaciers and ice sheets, Reviews of Geophysics, 15, 235–247, https://doi.org/10.1029/RG015i002p00235, 1977.

Cook, C. P., Van De Flierdt, T., Williams, T., Hemming, S. R., Iwai, M., Kobayashi, M., Jimenez-Espejo, F. J., Escutia, C., González, J. J., Khim, B.-K., et al.: Dynamic behaviour of the East Antarctic ice sheet during Pliocene warmth, Nature Geoscience, 6, 765–769, https://doi.org/10.1038/ngeo1889, 2013.

Coulon, V., Bulthuis, K., Whitehouse, P. L., Sun, S., Haubner, K., Zipf, L., and Pattyn, F.: Contrasting response of West and East Antarctic ice sheets to glacial isostatic adjustment, Journal of Geophysical Research: Earth Surface, 126, e2020JF006 003, https://doi.org/10.1029/2020JF006003, 2021.

Coulon, V., Klose, A. K., Kittel, C., Edwards, T., Turner, F., Winkelmann, R., and Pattyn, F.: Disentangling the drivers of future Antarctic ice loss with a historically-calibrated ice-sheet model, EGUsphere, 2023, 1–42, https://doi.org/10.5194/egusphere-2023-1532, 2023.

Cuffey, K. M. and Paterson, W. S. B.: The Physics of Glaciers, Academic Press, 2010.

DeConto, R. M. and Pollard, D.: Rapid Cenozoic glaciation of Antarctica induced by declining atmospheric CO2, Nature, 421, 245–249, https://doi.org/10.1038/nature01290, 2003.

DeConto, R. M. and Pollard, D.: Contribution of Antarctica to past and future sea-level rise, Nature, 531, 591–597, https://doi.org/10.1038/nature17145, 2016.

DeConto, R. M., Pollard, D., Alley, R. B., Velicogna, I., Gasson, E., Gomez, N., Sadai, S., Condron, A., Gilford, D. M., Ashe, E. L., et al.: The Paris Climate Agreement and future sea-level rise from Antarctica, Nature, 593, 83–89, https://doi.org/10.1038/s41586-021-03427-0, 2021.

Favier, L., Durand, G., Cornford, S. L., Gudmundsson, G. H., Gagliardini, O., Gillet-Chaulet, F., Zwinger, T., Payne, A., and Le Brocq, A. M.: Retreat of Pine Island Glacier controlled by marine ice-sheet instability, Nature Climate Change, 4, 117–121, https://doi.org/10.1038/nclimate2094, 2014.

https://doi.org/10.5194/tc-2023-156
Preprint. Discussion started: 9 October 2023

Feldmann, J., Albrecht, T., Khroulev, C., Pattyn, F., and Levermann, A.: Resolution-dependent performance of grounding line motion in a shallow model compared with a full-Stokes model according to the MISMIP3d intercomparison, Journal of Glaciology, 60, 353–360, https://doi.org/10.3189/2014JoG13J093, 2014.

Fox-Kemper, B., Hewitt, H., Xiao, C., Aðalgeirsdóttir, G., Drijfhout, S., Edwards, T., Golledge, N., Hemer, M., Kopp, R., Krinner, G., Mix, A., Notz, D., Nowicki, S., Nurhati, I., Ruiz, L., Sallée, J.-B., Slangen, A., and Yu, Y.: Ocean, Cryosphere and Sea Level Change. In Climate Change 2021: The Physical Science Basis. Contribution of Working Group I to the Sixth Assessment Report of the Intergovernmental Panel on Climate Change [Masson-Delmotte, V., P. Zhai, A. Pirani, S.L. Connors, C. Péan, S. Berger, N. Caud, Y. Chen, L. Goldfarb, M.I. Gomis, M. Huang, K. Leitzell, E. Lonnoy, J.B.R. Matthews, T.K. Maycock, T. Waterfield, O. Yelekçi, R. Yu, and B. Zhou (eds.)], Cambridge University Press, pp. 1211–1362, 2021.

Fretwell, P., Pritchard, H. D., Vaughan, D. G., Bamber, J. L., Barrand, N. E., Bell, R., Bianchi, C., Bingham, R., Blankenship, D. D., Casassa, G., et al.: Bedmap2: improved ice bed, surface and thickness datasets for Antarctica, The Cryosphere, 7, 375–393, https://doi.org/10.5194/tc-7-375-2013, 2013.

Fyke, J., Sergienko, O., Löfverström, M., Price, S., and Lenaerts, J. T.: An overview of interactions and feedbacks between ice sheets and the Earth system, Reviews of Geophysics, 56, 361–408, https://doi.org/10.1029/2018RG000600, 2018.

Garbe, J., Albrecht, T., Levermann, A., Donges, J. F., and Winkelmann, R.: The hysteresis of the Antarctic Ice Sheet, Nature, 585, 538–544, https://doi.org/10.1038/s41586-020-2727-5, 2020.

Garbe, J., Zeitz, M., Krebs-Kanzow, U., and Winkelmann, R.: The evolution of future Antarctic surface melt using PISM-dEBM-simple, The Cryosphere Discussions, pp. 1–39, 2023.

Golledge, N., Levy, R., McKay, R., and Naish, T.: East Antarctic ice sheet most vulnerable to Weddell Sea warming, Geophysical Research Letters, 44, 2343–2351, https://doi.org/10.1002/2016GL072422, 2017.

Golledge, N. R., Kowalewski, D. E., Naish, T. R., Levy, R. H., Fogwill, C. J., and Gasson, E. G.: The multi-millennial Antarctic commitment to future sea-level rise, Nature, 526, 421–425, https://doi.org/10.1038/nature15706, 2015.

Golledge, N. R., Keller, E. D., Gomez, N., Naughten, K. A., Bernales, J., Trusel, L. D., and Edwards, T. L.: Global environmental consequences of twenty-first-century ice-sheet melt, Nature, 566, 65–72, https://doi.org/10.1038/s41586-019-0889-9, 2019.

Golledge, N. R., Clark, P. U., He, F., Dutton, A., Turney, C., Fogwill, C., Naish, T., Levy, R. H., McKay, R. M., Lowry, D. P., et al.: Retreat of the Antarctic Ice Sheet during the Last Interglaciation and implications for future change, Geophysical Research Letters, 48, e2021GL094 513, https://doi.org/10.1029/2021GL094513, 2021.

Goosse, H., Brovkin, V., Fichefet, T., Haarsma, R., Huybrechts, P., Jongma, J., Mouchet, A., Selten, F., Barriat, P.-Y., Campin, J.-M., Deleersnijder, E., Driesschaert, E., Goelzer, H., Janssens, I., Loutre, M.-F., Morales Maqueda, M. A., Opsteegh, T., Mathieu, P.-P., Munhoven, G., Pettersson, E. J., Renssen, H., Roche, D. M., Schaeffer, M., Tartinville, B., Timmermann, A., and Weber, S. L.: Description of the Earth system model of intermediate complexity LOVECLIM version 1.2, Geoscientific Model Development, 3, 603–633, https://doi.org/10.5194/gmd-3-603-2010, 2010.

Gudmundsson, G. H., Krug, J., Durand, G., Favier, L., and Gagliardini, O.: The stability of grounding lines on retrograde slopes, The Cryosphere, 6, 1497–1505, https://doi.org/10.5194/tc-6-1497-2012, 2012.

Gulev, S., Thorne, P., Ahn, J., Dentener, F., Domingues, C., Gerland, S., Gong, D., Kaufman, D., Nnamchi, H., Quaas, J., Rivera, J., Sathyendranath, S., Smith, S., Trewin, B., von Schuckmann, K., and Vose, R.: Changing State of the Climate System. In Climate Change 2021: The Physical Science Basis. Contribution of Working Group I to the Sixth Assessment Report of the Intergovernmental Panel on Climate Change [Masson-Delmotte, V., P. Zhai, A. Pirani, S.L. Connors, C. Péan, S. Berger, N. Caud, Y. Chen, L. Goldfarb, M.I. Gomis,

M. Huang, K. Leitzell, E. Lonnoy, J.B.R. Matthews, T.K. Maycock, T. Waterfield, O. Yelekçi, R. Yu, and B. Zhou (eds.)], Cambridge University Press, p. 287–422, 2021.

Haseloff, M. and Sergienko, O. V.: The effect of buttressing on grounding line dynamics, Journal of Glaciology, 64, 417–431, https://doi.org/10.1017/jog.2018.30, 2018.

Haseloff, M. and Sergienko, O. V.: Effects of calving and submarine melting on steady states and stability of buttressed marine ice sheets, Journal of Glaciology, p. 1–18, https://doi.org/10.1017/jog.2022.29, 2022.

Huybrechts, P. and De Wolde, J.: The dynamic response of the Greenland and Antarctic ice sheets to multiple-century climatic warming, Journal of Climate, 12, 2169–2188, https://doi.org/10.1175/1520-0442(1999)012<2169:TDROTG>2.0.CO;2, 1999.

Jakobs, C. L., Reijmer, C. H., Kuipers Munneke, P., König-Langlo, G., and Van Den Broeke, M. R.: Quantifying the snowmelt–albedo feedback at Neumayer Station, East Antarctica, The Cryosphere, 13, 1473–1485, https://doi.org/10.5194/tc-13-1473-2019, 2019.

Jakobs, C. L., Reijmer, C. H., van den Broeke, M. R., Van de Berg, W., and Van Wessem, J.: Spatial Variability of the Snowmelt-Albedo Feedback in Antarctica, Journal of Geophysical Research: Earth Surface, 126, e2020JF005 696, https://doi.org/10.1029/2020JF005696, 2021.

Jenkins, A., Shoosmith, D., Dutrieux, P., Jacobs, S., Kim, T. W., Lee, S. H., Ha, H. K., and Stammerjohn, S.: West Antarctic Ice Sheet retreat in the Amundsen Sea driven by decadal oceanic variability, Nature Geoscience, 11, 733–738, https://doi.org/10.1038/s41561-018-0207-4, 2018.

Joughin, I., Smith, B. E., and Medley, B.: Marine ice sheet collapse potentially under way for the Thwaites Glacier Basin, West Antarctica, Science, 344, 735–738, https://doi.org/10.1126/science.1249055, 2014.

Kittel, C., Amory, C., Agosta, C., Jourdain, N. C., Hofer, S., Delhasse, A., Doutreloup, S., Huot, P.-V., Lang, C., Fichefet, T., and Fettweis, X.: Diverging future surface mass balance between the Antarctic ice shelves and grounded ice sheet, The Cryosphere, 15, 1215–1236, https://doi.org/10.5194/tc-15-1215-2021, 2021.

Kreuzer, M., Reese, R., Huiskamp, W. N., Petri, S., Albrecht, T., Feulner, G., and Winkelmann, R.: Coupling framework (1.0) for the PISM (1.1.4) ice sheet model and the MOM5 (5.1.0) ocean model via the PICO ice shelf cavity model in an Antarctic domain, Geoscientific Model Development, 14, 3697–3714, https://doi.org/10.5194/gmd-14-3697-2021, 2021.

Le Meur, E. and Huybrechts, P.: A comparison of different ways of dealing with isostasy: examples from modelling the Antarctic ice sheet during the last glacial cycle, Annals of Glaciology, 23, 309–317, https://doi.org/10.3189/S0260305500013586, 1996.

Lee, J.-Y., Marotzke, J., Bala, G., Cao, L., Corti, S., Dunne, J., Engelbrecht, F., Fischer, E., Fyfe, J., Jones, C., Maycock, A., Mutemi, J., Ndiaye, O., Panickal, S., and Zhou, T.: Future Global Climate: Scenario-Based Projections and Near- Term Information. In Climate Change 2021: The Physical Science Basis. Contribution of Working Group I to the Sixth Assessment Report of the Intergovernmental Panel on Climate Change [Masson-Delmotte, V., P. Zhai, A. Pirani, S.L. Connors, C. Péan, S. Berger, N. Caud, Y. Chen, L. Goldfarb, M.I. Gomis, M. Huang, K. Leitzell, E. Lonnoy, J.B.R. Matthews, T.K. Maycock, T. Waterfield, O. Yelekçi, R. Yu, and B. Zhou (eds.)], Cambridge University Press, pp. 553–672, 2021.

Lenton, T. M., Held, H., Kriegler, E., Hall, J. W., Lucht, W., Rahmstorf, S., and Schellnhuber, H. J.: Tipping elements in the Earth's climate system, Proceedings of the National Academy of Sciences, 105, 1786–1793, https://doi.org/10.1073/pnas.0705414105, 2008.

Levermann, A. and Winkelmann, R.: A simple equation for the melt elevation feedback of ice sheets, The Cryosphere, 10, 1799–1807, https://doi.org/10.5194/tc-10-1799-2016, 2016.

Levermann, A., Albrecht, T., Winkelmann, R., Martin, M. A., Haseloff, M., and Joughin, I.: Kinematic first-order calving law implies potential for abrupt ice-shelf retreat, The Cryosphere, 6, 273–286, https://doi.org/10.5194/tc-6-273-2012, 2012.

Levy, R., Harwood, D., Florindo, F., Sangiorgi, F., Tripati, R., Von Eynatten, H., Gasson, E., Kuhn, G., Tripati, A., DeConto, R., et al.: Antarctic ice sheet sensitivity to atmospheric CO2 variations in the early to mid-Miocene, Proceedings of the National Academy of Sciences, 113, 3453–3458, https://doi.org/10.1073/pnas.1516030113, 2016.

Li, C., von Storch, J.-S., and Marotzke, J.: Deep-ocean heat uptake and equilibrium climate response, Climate Dynamics, 40, 1071–1086, https://doi.org/10.1007/s00382-012-1350-z, 2013.

Li, X., Rignot, E., Mouginot, J., and Scheuchl, B.: Ice flow dynamics and mass loss of Totten Glacier, East Antarctica, from 1989 to 2015, Geophysical Research Letters, 43, 6366–6373, https://doi.org/10.1002/2016GL069173, 2016.

Lingle, C. S. and Clark, J. A.: A numerical model of interactions between a marine ice sheet and the solid earth: Application to a West Antarctic ice stream, Journal of Geophysical Research: Oceans, 90, 1100–1114, https://doi.org/10.1029/JC090iC01p01100, 1985.

Lowry, D. P., Krapp, M., Golledge, N. R., and Alevropoulos-Borrill, A.: The influence of emissions scenarios on future Antarctic ice loss is unlikely to emerge this century, Communications Earth & Environment, 2, 1–14, 2021.

Martin, M. A., Winkelmann, R., Haseloff, M., Albrecht, T., Bueler, E., Khroulev, C., and Levermann, A.: The Potsdam Parallel Ice Sheet Model (PISM-PIK)–Part 2: dynamic equilibrium simulation of the Antarctic ice sheet, The Cryosphere, 5, 727–740, https://doi.org/10.5194/tc-5-727-2011, 2011.

Meehl, G. A., Senior, C. A., Eyring, V., Flato, G., Lamarque, J.-F., Stouffer, R. J., Taylor, K. E., and Schlund, M.: Context for interpreting equilibrium climate sensitivity and transient climate response from the CMIP6 Earth system models, Science Advances, 6, eaba1981, https://doi.org/10.1126/sciadv.aba1981, 2020.

Mengel, M. and Levermann, A.: Ice plug prevents irreversible discharge from East Antarctica, Nature Climate Change, 4, 451–455, https://doi.org/10.1038/nclimate2226, 2014.

Merz, N., Gfeller, G., Born, A., Raible, C., Stocker, T., and Fischer, H.: Influence of ice sheet topography on Greenland precipitation during the Eemian interglacial, Journal of Geophysical Research: Atmospheres, 119, 10–749, https://doi.org/10.1002/2014JD021940, 2014.

Mikkelsen, T. B., Grinsted, A., and Ditlevsen, P.: Influence of temperature fluctuations on equilibrium ice sheet volume, The Cryosphere, 12, 39–47, https://doi.org/10.5194/tc-12-39-2018, 2018.

Miles, B. W., Jordan, J. R., Stokes, C. R., Jamieson, S. S., Gudmundsson, G. H., and Jenkins, A.: Recent acceleration of Denman Glacier (1972–2017), East Antarctica, driven by grounding line retreat and changes in ice tongue configuration, The Cryosphere, 15, 663–676, https://doi.org/10.5194/tc-15-663-2021, 2021.

Morlighem, M., Rignot, E., Binder, T., Blankenship, D., Drews, R., Eagles, G., Eisen, O., Ferraccioli, F., Forsberg, R., Fretwell, P., et al.: Deep glacial troughs and stabilizing ridges unveiled beneath the margins of the Antarctic ice sheet, Nature Geoscience, 13, 132–137, https://doi.org/10.1038/s41561-019-0510-8, 2020.

Mottram, R., Hansen, N., Kittel, C., van Wessem, J. M., Agosta, C., Amory, C., Boberg, F., van de Berg, W. J., Fettweis, X., Gossart, A., et al.: What is the surface mass balance of Antarctica? An intercomparison of regional climate model estimates, The Cryosphere, 15, 3751–3784, https://doi.org/10.5194/tc-15-3751-2021, 2021.

Naish, T., Powell, R., Levy, R., Wilson, G., Scherer, R., Talarico, F., Krissek, L., Niessen, F., Pompilio, M., Wilson, T., et al.: Obliquity-paced Pliocene West Antarctic ice sheet oscillations, Nature, 458, 322–328, https://doi.org/10.1038/nature07867, 2009.

Naish, T. R., Woolfe, K. J., Barrett, P. J., Wilson, G. S., Atkins, C., Bohaty, S. M., Bücker, C. J., Claps, M., Davey, F. J., Dunbar, G. B., et al.: Orbitally induced oscillations in the East Antarctic ice sheet at the Oligocene/Miocene boundary, Nature, 413, 719–723, https://doi.org/10.1038/35099534, 2001.

https://doi.org/10.5194/tc-2023-156
Preprint. Discussion started: 9 October 2023

Nias, I. J., Cornford, S. L., and Payne, A. J.: Contrasting the modelled sensitivity of the Amundsen Sea Embayment ice streams, Journal of Glaciology, 62, 552–562, https://doi.org/10.1017/jog.2016.40, 2016.

Nowicki, S., Goelzer, H., Seroussi, H., Payne, A. J., Lipscomb, W. H., Abe-Ouchi, A., Agosta, C., Alexander, P., Asay-Davis, X. S., Barthel, A., Bracegirdle, T. J., Cullather, R., Felikson, D., Fettweis, X., Gregory, J. M., Hattermann, T., Jourdain, N. C., Kuipers Munneke, P., Larour, E., Little, C. M., Morlighem, M., Nias, I., Shepherd, A., Simon, E., Slater, D., Smith, R. S., Straneo, F., Trusel, L. D., van den Broeke, M. R., and van de Wal, R.: Experimental protocol for sea level projections from ISMIP6 stand-alone ice sheet models, The Cryosphere, 14, 2331–2368, https://doi.org/10.5194/tc-14-2331-2020, 2020.

Oerlemans, J.: Some basic experiments with a vertically-integrated ice sheet model, Tellus, 33, 1–11, https://doi.org/10.3402/tellusa.v33i1.10690, 1981.

O'Neill, B. C., Tebaldi, C., Van Vuuren, D. P., Eyring, V., Friedlingstein, P., Hurtt, G., Knutti, R., Kriegler, E., Lamarque, J.-F., Lowe, J., et al.: The scenario model intercomparison project (ScenarioMIP) for CMIP6, Geoscientific Model Development, 9, 3461–3482, https://doi.org/10.5194/gmd-9-3461-2016, 2016.

Otosaka, I. N., Shepherd, A., Ivins, E. R., Schlegel, N.-J., Amory, C., van den Broeke, M. R., Horwath, M., Joughin, I., King, M. D., Krinner, G., Nowicki, S., Payne, A. J., Rignot, E., Scambos, T., Simon, K. M., Smith, B. E., Sørensen, L. S., Velicogna, I., Whitehouse, P. L., A, G., Agosta, C., Ahlstrøm, A. P., Blazquez, A., Colgan, W., Engdahl, M. E., Fettweis, X., Forsberg, R., Gallée, H., Gardner, A., Gilbert, L., Gourmelen, N., Groh, A., Gunter, B. C., Harig, C., Helm, V., Khan, S. A., Kittel, C., Konrad, H., Langen, P. L., Lecavalier, B. S., Liang, C.-C., Loomis, B. D., McMillan, M., Melini, D., Mernild, S. H., Mottram, R., Mouginot, J., Nilsson, J., Noël, B., Pattle, M. E., Peltier, W. R., Pie, N., Roca, M., Sasgen, I., Save, H. V., Seo, K.-W., Scheuchl, B., Schrama, E. J. O., Schröder, L., Simonsen, S. B., Slater, T., Spada, G., Sutterley, T. C., Vishwakarma, B. D., van Wessem, J. M., Wiese, D., van der Wal, W., and Wouters, B.: Mass balance of the Greenland and Antarctic ice sheets from 1992 to 2020, Earth System Science Data, 15, 1597–1616, https://doi.org/10.5194/essd-15-1597-2023, 2023.

Paolo, F., Padman, L., Fricker, H., Adusumilli, S., Howard, S., and Siegfried, M.: Response of Pacific-sector Antarctic ice shelves to the El Niño/Southern oscillation, Nature geoscience, 11, 121–126, 2018.

Paolo, F. S., Fricker, H. A., and Padman, L.: Volume loss from Antarctic ice shelves is accelerating, Science, 348, 327–331, https://doi.org/10.1126/science.aaa0940, 2015.

Patterson, M. O., McKay, R., Naish, T., Escutia, C., Jimenez-Espejo, F., Raymo, M., Meyers, S., Tauxe, L., and Brinkhuis, H.: Orbital forcing of the East Antarctic ice sheet during the Pliocene and Early Pleistocene, Nature Geoscience, 7, 841–847, https://doi.org/10.1038/ngeo2273, 2014.

Pattyn, F.: Sea-level response to melting of Antarctic ice shelves on multi-centennial timescales with the fast Elementary Thermomechanical Ice Sheet model (f.ETISh v1.0), The Cryosphere, 11, 1851–1878, https://doi.org/10.5194/tc-11-1851-2017, 2017.

Pattyn, F., Perichon, L., Durand, G., Favier, L., Gagliardini, O., Hindmarsh, R. C., Zwinger, T., Albrecht, T., Cornford, S., Docquier, D., and et al.: Grounding-line migration in plan-view marine ice-sheet models: results of the ice2sea MISMIP3d intercomparison, Journal of Glaciology, 59, 410–422, https://doi.org/10.3189/2013JoG12J129, 2013.

Payne, A. J., Nowicki, S., Abe-Ouchi, A., Agosta, C., Alexander, P., Albrecht, T., Asay-Davis, X., Aschwanden, A., Barthel, A., Bracegirdle, T. J., et al.: Future sea level change under Coupled Model Intercomparison Project Phase 5 and Phase 6 scenarios from the Greenland and Antarctic ice sheets, Geophysical Research Letters, 48, e2020GL091 741, https://doi.org/10.1029/2020GL091741, 2021.

Pegler, S. S.: Marine ice sheet dynamics: the impacts of ice-shelf buttressing, Journal of Fluid Mechanics, 857, 605–647, https://doi.org/10.1038/s41561-017-0033-0, 2018.

https://doi.org/10.5194/tc-2023-156
Preprint. Discussion started: 9 October 2023

Pollard, D. and DeConto, R. M.: Modelling West Antarctic ice sheet growth and collapse through the past five million years, Nature, 458, 329–332, https://doi.org/10.1038/nature07809, 2009.

Pollard, D. and DeConto, R. M.: Description of a hybrid ice sheet-shelf model, and application to Antarctica, Geoscientific Model Development, 5, 1273–1295, https://doi.org/10.5194/gmd-5-1273-2012, 2012a.

Pollard, D. and DeConto, R. M.: A simple inverse method for the distribution of basal sliding coefficients under ice sheets, applied to Antarctica, The Cryosphere, 6, 953–971, https://doi.org/10.5194/tc-6-953-2012, 2012b.

Pollard, D. and DeConto, R. M.: Improvements in one-dimensional grounding-line parameterizations in an ice-sheet model with lateral variations (PSUICE3D v2.1), Geoscientific Model Development, 13, 6481–6500, https://doi.org/10.5194/gmd-13-6481-2020, 2020.

Pollard, D., DeConto, R. M., and Alley, R. B.: Potential Antarctic Ice Sheet retreat driven by hydrofracturing and ice cliff failure, Earth and Planetary Science Letters, 412, 112–121, https://doi.org/10.1016/j.epsl.2014.12.035, 2015.

Purich, A. and England, M. H.: Historical and future projected warming of Antarctic Shelf Bottom Water in CMIP6 models, Geophysical Research Letters, 48, e2021GL092 752, https://doi.org/10.1029/2021GL092752, 2021.

Reeh, N.: Parameterization of melt rate and surface temperature on the Greenland ice sheet, Polarforschung, 59, 113–128, 1991.

Reese, R., Albrecht, T., Mengel, M., Asay-Davis, X., and Winkelmann, R.: Antarctic sub-shelf melt rates via PICO, The Cryosphere, 12, 1969–1985, https://doi.org/10.5194/tc-12-1969-2018, 2018.

Reese, R., Levermann, A., Albrecht, T., Seroussi, H., and Winkelmann, R.: The role of history and strength of the oceanic forcing in sea level projections from Antarctica with the Parallel Ice Sheet Model, The Cryosphere, 14, 3097–3110, https://doi.org/10.5194/tc-14-3097-2020, 2020.

Reese, R., Garbe, J., Hill, E. A., Urruty, B., Naughten, K. A., Gagliardini, O., Durand, G., Gillet-Chaulet, F., Gudmundsson, G. H., Chandler, D., et al.: The stability of present-day Antarctic grounding lines–Part 2: Onset of irreversible retreat of Amundsen Sea glaciers under current climate on centennial timescales cannot be excluded, The Cryosphere, 17, 3761–3783, https://doi.org/10.5194/tc-17-3761-2023, 2023.

Rignot, E., Mouginot, J., and Scheuchl, B.: Ice flow of the Antarctic Ice Sheet, Science, 333, 1427–1430, https://doi.org/10.1126/science.1208336, 2011.

Rignot, E., Mouginot, J., Scheuchl, B., Van Den Broeke, M., Van Wessem, M. J., and Morlighem, M.: Four decades of Antarctic Ice Sheet mass balance from 1979–2017, Proceedings of the National Academy of Sciences, 116, 1095–1103, https://doi.org/10.1073/pnas.1812883116, 2019.

Ritchie, P. D., Clarke, J. J., Cox, P. M., and Huntingford, C.: Overshooting tipping point thresholds in a changing climate, Nature, 592, 517–523, https://doi.org/10.1038/s41586-021-03263-2, 2021.

Robel, A. A., Seroussi, H., and Roe, G. H.: Marine ice sheet instability amplifies and skews uncertainty in projections of future sea-level rise, Proceedings of the National Academy of Sciences, 116, 14 887–14 892, https://doi.org/10.1073/pnas.1904822116, 2019.

Robinson, A., Calov, R., and Ganopolski, A.: Multistability and critical thresholds of the Greenland ice sheet, Nature Climate Change, 2, 429–432, https://doi.org/10.1038/nclimate1449, 2012.

Rosier, S. H., Reese, R., Donges, J. F., De Rydt, J., Gudmundsson, G. H., and Winkelmann, R.: The tipping points and early warning indicators for Pine Island Glacier, West Antarctica, The Cryosphere, 15, 1501–1516, https://doi.org/10.5194/tc-15-1501-2021, 2021.

Schmidtko, S., Heywood, K. J., Thompson, A. F., and Aoki, S.: Multidecadal warming of Antarctic waters, Science, 346, 1227–1231, https://doi.org/10.1126/science.1256117, 2014.

Schoof, C.: Ice sheet grounding line dynamics: Steady states, stability, and hysteresis, Journal of Geophysical Research: Earth Surface, 112, https://doi.org/10.1029/2006JF000664, 2007.

Sergienko, O. V.: No general stability conditions for marine ice-sheet grounding lines in the presence of feedbacks, Nature Communications, 13, 2265, https://doi.org/10.1038/s41467-022-29892-3, 2022.

Seroussi, H., Nakayama, Y., Larour, E., Menemenlis, D., Morlighem, M., Rignot, E., and Khazendar, A.: Continued retreat of Thwaites Glacier, West Antarctica, controlled by bed topography and ocean circulation, Geophysical Research Letters, 44, 6191–6199, https://doi.org/10.1002/2017GL072910, 2017.

Seroussi, H., Nowicki, S., Simon, E., Abe-Ouchi, A., Albrecht, T., Brondex, J., Cornford, S., Dumas, C., Gillet-Chaulet, F., Goelzer, H., et al.: initMIP-Antarctica: an ice sheet model initialization experiment of ISMIP6, The Cryosphere, 13, 1441–1471, https://doi.org/10.5194/tc-13-1441-2019, 2019.

Seroussi, H., Nowicki, S., Payne, A. J., Goelzer, H., Lipscomb, W. H., Abe-Ouchi, A., Agosta, C., Albrecht, T., Asay-Davis, X., Barthel, A., et al.: ISMIP6 Antarctica: a multi-model ensemble of the Antarctic ice sheet evolution over the 21st century, The Cryosphere, 14, 3033–3070, https://doi.org/10.5194/tc-14-3033-2020, 2020.

Shakun, J. D., Corbett, L. B., Bierman, P. R., Underwood, K., Rizzo, D. M., Zimmerman, S. R., Caffee, M. W., Naish, T., Golledge, N. R., and Hay, C. C.: Minimal East Antarctic Ice Sheet retreat onto land during the past eight million years, Nature, 558, 284–287, https://doi.org/10.1038/s41586-018-0155-6, 2018.

Sugden, D. E., Marchant, D. R., Potter, N., Souchez, R. A., Denton, G. H., Swisher III, C. C., and Tison, J.-L.: Preservation of Miocene glacier ice in East Antarctica, Nature, 376, 412–414, https://doi.org/10.1038/376412a0, 1995.

Sun, S., Pattyn, F., Simon, E. G., Albrecht, T., Cornford, S., Calov, R., Dumas, C., Gillet-Chaulet, F., Goelzer, H., Golledge, N. R., and et al.: Antarctic ice sheet response to sudden and sustained ice-shelf collapse (ABUMIP), Journal of Glaciology, p. 891–904, https://doi.org/0.1017/jog.2020.67, 2020.

Tokarska, K. B., Zickfeld, K., and Rogelj, J.: Path independence of carbon budgets when meeting a stringent global mean temperature target after an overshoot, Earth's Future, 7, 1283–1295, https://doi.org/10.1029/2019EF001312, 2019.

Turney, C. S., Fogwill, C. J., Golledge, N. R., McKay, N. P., van Sebille, E., Jones, R. T., Etheridge, D., Rubino, M., Thornton, D. P., Davies, S. M., et al.: Early Last Interglacial ocean warming drove substantial ice mass loss from Antarctica, Proceedings of the National Academy of Sciences, 117, 3996–4006, https://doi.org/10.1073/pnas.1902469117, 2020.

Van Breedam, J., Goelzer, H., and Huybrechts, P.: Semi-equilibrated global sea-level change projections for the next 10 000 years, Earth System Dynamics, 11, 953–976, https://doi.org/10.5194/esd-11-953-2020, 2020.

Van Wessem, J. M., Van De Berg, W. J., Noël, B. P., Van Meijgaard, E., Amory, C., Birnbaum, G., Jakobs, C. L., Krüger, K., Lenaerts, J., Lhermitte, S., et al.: Modelling the climate and surface mass balance of polar ice sheets using RACMO2–Part 2: Antarctica (1979–2016), The Cryosphere, 12, 1479–1498, https://doi.org/10.5194/tc-12-1479-2018, 2018.

Weber, M., Clark, P., Kuhn, G., Timmermann, A., Sprenk, D., Gladstone, R., Zhang, X., Lohmann, G., Menviel, L., Chikamoto, M., et al.: Millennial-scale variability in Antarctic ice-sheet discharge during the last deglaciation, Nature, 510, 134–138, https://doi.org/10.1038/nature13397, 2014.

Weertman, J.: Stability of the junction of an ice sheet and an ice shelf, Journal of Glaciology, 13, 3–11, https://doi.org/10.3189/S0022143000023327, 1974.

https://doi.org/10.5194/tc-2023-156
Preprint. Discussion started: 9 October 2023

Wilson, D. J., Bertram, R. A., Needham, E. F., van de Flierdt, T., Welsh, K. J., McKay, R. M., Mazumder, A., Riesselman, C. R., Jimenez-Espejo, F. J., and Escutia, C.: Ice loss from the East Antarctic Ice Sheet during late Pleistocene interglacials, Nature, 561, 383–386, https://doi.org/10.1038/s41586-018-0501-8, 2018.

Winkelmann, R., Martin, M. A., Haseloff, M., Albrecht, T., Bueler, E., Khroulev, C., and Levermann, A.: The Potsdam Parallel Ice Sheet Model (PISM-PIK)–Part 1: Model description, The Cryosphere, 5, 715–726, https://doi.org/10.5194/tc-5-715-2011, 2011.

Winkelmann, R., Levermann, A., Ridgwell, A., and Caldeira, K.: Combustion of available fossil fuel resources sufficient to eliminate the Antarctic Ice Sheet, Science Advances, 1, e1500 589, https://doi.org/10.1126/sciadv.1500589, 2015.

Zachos, J., Pagani, M., Sloan, L., Thomas, E., and Billups, K.: Trends, rhythms, and aberrations in global climate 65 Ma to present, Science, 292, 686–693, https://doi.org/10.1126/science.1059412, 2001.

Zeitz, M., Reese, R., Beckmann, J., Krebs-Kanzow, U., and Winkelmann, R.: Impact of the melt–albedo feedback on the future evolution of the Greenland Ice Sheet with PISM-dEBM-simple, The Cryosphere, 15, 5739–5764, https://doi.org/10.5194/tc-15-5739-2021, 2021.

Zhu, J., Otto-Bliesner, B. L., Brady, E. C., Poulsen, C. J., Tierney, J. E., Lofverstrom, M., and DiNezio, P.: Assessment of equilibrium climate sensitivity of the Community Earth System Model version 2 through simulation of the Last Glacial Maximum, Geophysical Research Letters, 48, e2020GL091 220, https://doi.org/10.1029/2020GL091220, 2021.